FLOW FIELD AROUND A FINITE CONE WITH SHOCK

Thesis by

Lt. Comdr. Neil A. Mac Kinnon, USN

In Partial Fulfillment of the Requirements

for the Degree of Aeronautical Engineer

California Institute of Technology

Pasadena, California

1949

ABSTRACT

An experimental investigation was made to determine the characteristics of the flow over the surface of a 70° cone and at the shock wave for values near the detachment Mach number. The purpose of this investigation was to compare the experimental results obtained with theoretical values.

Tests were made in the GALCIT 2.5" Supersonic Wind Tunnel on a 70° cone at zero angle of attack for five different free stream Mach numbers: 1.49, 1.630, 1.694, 1.86, 1.997.

It was found that theory gives close agreement with experimental results.

This investigation was conducted jointly with Mr. Vincent Muirhead at the California Institute of Technology, Pasadena, California.

ACKNOWLEDGMENTS

This investigation was conducted jointly with Mr. Vincent Muirhead. Appreciation is expressed to Mr. Allen E. Puckett and Mr. Henry Nagamatsu for their advice and assistance.

TABLE OF CONTENTS

Part	Title	Page
	Abstract	i
	Acknowledgments	ii
	Table of Contents	iii
	List of Figures	iv
I.	Introduction	1
II.	Equipment and Procedure	4
III.	Results and Discussion	6
IV.	Conclusions	10
	References	11
	Sample Calculations	12
	Figures	15

LIST OF FIGURES

Figure No.	Subject	Page
1	Cone Pressure Models	15
2	Centerline Survey	16
3	Determination of Angle of Attack	17
4	Symbols	18
5	70° Cone-Pressure Distribution M = 1.49, P_s/P_o	19
6	" " " " M = 1.636 "	20
7	" " " " M = 1.694 "	21
8	" " " " M = 1.86 "	22
9	" " " " M = 1.997 "	23
10	" " " " (Summary) "	24
11	" " " " (Orifice) "	25
12	" " " " M = 1.49 P_s/P_o	26
13	" " " " M = 1.636 "	27
14	" " " " M = 1.694 "	28
15	" " " " M = 1.86 "	29
16	" " " " M = 1.997 "	30
17	" " " " (Summary) "	31
18	" " " " (Orifice) "	32
19	70° Cone-Shock Wave Pattern	33
20	70° Cone-Shock Wave Angle and M_2, M = 1.49	34
21	" " " " " " " M = 1.636	35
22	" " " " " " " M = 1.694	36
23	" " " " " " " M = 1.86	37
24	" " " " " " " M = 1.997	38

LIST OF FIGURES

Figure No.	Subject	Page
25	70° Cone-Shock Wave Angle (Summary)	39
26	70° Cone-Mach Number Behind Shock (Summary)	40
27	70° Cone-Theoretical Surface Pressure	41
28	70° Cone-Theoretical Shock Wave Angle	42
29	Schlieren Picture, M = 1.49	43
30	" " M = 1.636	44
31	" " M = 1.636 (Enlarged)	45
32	" " M = 1.694	46
33	" " M = 1.694 (Enlarged)	47
34	" " M = 1.86	48
35	" " M = 1.997	49

I. INTRODUCTION

The purpose of this investigation was to determine experimentally the characteristics of the flow over the surface of a 70° cone and at the shock wave for values near the detachment Mach number. A further purpose was to compare the experimental results obtained with values determined analytically for an infinite 70° cone.

A previous experimental investigation of this problem by Marschner and Altseimer (Ref. 1) was inconclusive for points near the apex of the cone. In addition, the Marschner and Altseimer work was not directly comparable with analytical results since no analytical data were available for the exact cone angle which they used.

In this investigation only the flow parameters at the surface of the model and the configuration of the primary shock wave were determined. A 70° cone with a circular cylindrical afterbody was tested at zero angle of attack. Tests were made at five different Mach numbers: 1.49, 1.636, 1.694, 1.86, 1.997.

Theory predicts that the initial Mach number for which the shock wave first becomes attached to the cone is 1.681. The free stream Mach number at which the flow theoretically first attains sonic velocity behind the shock wave is 1.769. The initial Mach number for which the flow theoretically first becomes sonic along the surface of the cone is 1.911. Mach 1.49 therefore was chosen to give a well defined detached shock. Mach 1.636 was chosen to give a detached shock under conditions very slightly removed from those at attachment. Mach 1.694 was selected to give an

attached shock close to the minimum Mach number for attachment where the flow after the shock was subsonic. Mach 1.86 was selected to give an attached shock with supersonic flow after the shock except for a region near the surface of the cone where the flow is subsonic. Mach 1.997 was chosen to give an attached shock with the flow after the shock supersonic including the region at the cone surface.

For the convenience of the reader, the above is recapitulated in tabuler form:

Initial Mach number used	Theoretical Min. Mach No. for condition described	Shock wave	Flow behind shock	Flow along cone surface
1.49	1.00	Detached	Subsonic	Subsonic
1.636	1.00	Detached	Subsonic	Subsonic
1.694	1.683	Attached	Subsonic	Subsonic
1.86	1.775	Attached	Supersonic	Subsonic
1.997	1.917	Attached	Supersonic	Supersonic

In order to improve on the results obtained by Marschner and Altseimer, the largest model possible without blocking the tunnel was used and a pressure orifice was placed as close to the nose as practicable. To make possible an exact comparison with theory a 70° cone angle was used since computed values are tabulated for that angle (Ref. 2).

The mathematical treatment of the problem of supersonic flows around infinite cones has been given by several investigators, notably Busemann

(Ref. 3) and Taylor and Maccoll (Ref. 4). Kopal has supplied computed numerical data based on the mathematical theory (Ref. 2). It is the aim of this work to compare this computed data with experimental data obtained.

This investigation was conducted in the 2.5" Supersonic Wind Tunnel at the Guggenheim Aeronautical Laboratory, California Institute of Technology, Pasadena, California during the winter of 1948-1949.

II. EQUIPMENT AND PROCEDURE

Eight models were tested. Each was a brass circular cylinder with a 70° conical nose and had one static pressure orifice at some point on the cone or cylinder. The models differed from each other only in the location of this pressure orifice. For details see Fig. 1.

The models were tested in the GALCIT 2.5" Supersonic Wind Tunnel. This is a single return, closed throat, continuous cycle wind tunnel with a 2.5" x 2.5" test section. For a detailed description of the tunnel see Ref. 5. The model was supported by a sting which could be adjusted in angle of attack, but not in yaw. Fixed steel nozzle blocks were used for Mach numbers 1.636 and 1.997. Flexible bronze nozzle blocks were used for Mach numbers 1.49, 1.694 and 1.86. The details of construction and method of adjusting the flexible nozzle blocks are contained in Ref. 1.

Photographs of the flow were taken with the standard Schlieren apparatus installed in this tunnel.

The Mach number variation in the test section (Fig. 2) was determined by a centerline pressure survey. Static pressure was taken from an orifice in a section of hypodermic tubing clamped in the axis of the nozzle and test section. The difference between the centerline pressure and the test section wall pressure was measured on an acetylene tetrabromide manometer. This pressure difference was added to the wall pressure measured against atmospheric pressure on a mercury manometer.

The model was set at zero angle of attack by the following procedure. Pressure readings were taken for two angles of attack with the orifice on top. Pressure readings for the same two angles of attack were then taken with the orifice on the bottom. A plot of pressure versus angle of attack was made (Fig. 3) and the intersection of the line for the orifice up with the line for the orifice down gave the zero angle of attack. This zero setting was checked both with the orifice up and the orifice down and adjusted until no variation existed.

Static pressure at the model orifice, settling tank pressure, and test section wall pressure were read on vertical U-tube mercury manometers against atmospheric pressure. Barometric pressure, room temperature and settling tank temperature were recorded.

To determine relative humidity, a sample of tunnel air was bled from the settling tank and passed over a cooled, polished, metal disc. The temperature at which condensation first occurred was taken as the dew point. From this the relative humidity was determined. The silica gel dryer in the tunnel air circuit kept the relative humidity in the range from .02 to .04.

III. RESULTS AND DISCUSSION

Fig. 4 is a graphical presentation of the notation employed.

Figs. 5 and 6 show the pressure distribution over the model for the case of the detached shock wave ($M = 1.49$ and $M = 1.636$). At the nose the curves are faired to the pressure which theoretically obtained behind a normal shock wave. This was felt to be a valid procedure since the photographs of the flow show a normal shock close to the nose and since the pressure climbs abruptly as the nose is approached. These results tend to clear up the uncertainty left by the Marschner experiment as to the behaviour close to the nose near the attachment Mach number.

After the large initial acceleration near the nose the flow accelerates uniformly but more slowly over the middle part of the cone face and then speeds up again near the corner of the cone and cylinder. The theoretical pressure at which the flow becomes sonic is indicated at the corner. The model and tunnel wall form an effective throat at which the flow becomes sonic.

Fig. 7 shows the case of the attached shock with subsonic flow behind the shock and along the cone face ($M = 1.694$). The theoretical pressure at the nose to which the curve is faired is that given in the Kopal report (Ref. 2). It appears from the plot that the flow attains sonic velocity at a point slightly ahead of the corner ($x/s = .975$).

Fig. 8 shows the conditions with mixed flow behind the attached shock ($M = 1.86$). Again the theoretical nose pressure is taken from

Kopal. It is indicated that the flow is subsonic over the first half of the cone and supersonic over the latter half.

Fig. 9 shows the pressure distribution with the whole field supersonic ($M = 1.997$). The flow along the entire cone face is nearly constant and in good agreement with the theoretical value as given in Kopal. The pressure for a Prandtl-Meyer expansion around the corner is indicated.

Fig. 10 is a summary which shows that the transition of the flow through the several regimes is remarkably gradual and even. The jump in pressure at detachment of the shock wave is apparently abrupt for only a very small portion of the flow field very close to the nose of the cone. It can also be seen that the flow field is conical only for the case where the flow behind the shock is everywhere supersonic ($M = 1.997$). Where there is mixed flow behind the shock, the flow is non-conical.

Fig. 11 shows the variation of pressure with Mach number for each orifice. The curves are regular except for a possible small discontinuity in slope at the attachment Mach number. The curves are dotted for this portion of the Mach spectrum.

Fig. 12 through 18 are similar to Figs. 5 through 11 described above except for the reference pressure used. In Figs. 5 through 11 the pressure was given in ratio to the settling tank pressure, p_o. In Figs. 12 through 18 the pressure is given in ratio to the theoretical reservoir pressure corresponding to condition behind the shock, p_o'. For the detached shock, normal shock wave relation were used. For the attached shocks, oblique shock wave relations were used

considering the shock angle existing at the nose.

Fig. 19 shows, to a scale six times actual size, the configuration of the primary shock waves for the various Mach numbers tested. These patterns were traced from projections of the Schlieren photographs taken.

Figs. 20 through 24 are plots of shock wave angle and Mach number after the shock. The wave angle was measured directly from the shock traces and the Mach number after the shock calculated from the oblique shock relations. The theoretical value for the wave angle for an infinite cone as derived from Kopal is indicated on the curves. Figs. 25 and 26 are summaries showing the gradual transition of the conditions at the shock through the different types of flow.

From Fig. 26 it can be seen that the point at which $M_2 = 1$ just behind the shock is:

Initial Mach number	Y/D at which $M_2 = 1$
1.49	.96
1.636	.83
1.694	.67

From this and the previously noted point at which M = 1 on the surface of the cone, we get two points on the boundary line between subsonic and supersonic flow.

Fig. 27 gives the theoretical surface pressure for an infinite 70° cone plotted against free stream Mach number. Fig. 28 gives the theoretical shock wave angle. In Fig. 28 the minimum Mach number at which

the flow behind the shock becomes supersonic and the minimum Mach number at which the flow over the surface of the cone becomes supersonic are indicated. Figs. 27 and 28 were plotted from data given by Kopal. Experimental points for the apex of the cone are superimposed on the theoretical curves.

Figs. 29 through 35 are Schlieren photographs of the models at various test Mach numbers.

The results in general show close agreement with theory in all details where direct comparisons are possible and are nowhere incompatible with theory. The results are also in agreement with the work of Marschner and Altseimer and amplify their results for points close to the apex of the cone.

IV. CONCLUSIONS

It is concluded that theory gives excellent agreement with experimental results for those values of flow compared. It is felt that this investigation is a good experimental check on the analytical data of the Kopal report (Ref. 2), and, by extension, that all values tabulated can be used with confidence.

It is further concluded that the transition from detached to attached shock wave proceeds smoothly and with no violent changes in the flow, except for a jump in the pressure at attachment at the extreme tip of the cone.

REFERENCES

1. Marschner, B. W., and Altseimer, J., "An Investigation of Detached Shock Waves", Thesis in partial fulfillment of the requirements for the Degree of Aeronautical Engineer, California Institute of Technology, 1948.

2. Kopal, Z., "Supersonic Flow Around Cones", Massachusetts Institute of Technology, Center of Analysis, Report No. 1, 1947.

3. Busemann, Von A., Zeitschrift fur Angewandte Mathematik und Mechanik, 2, 496, 1929, "Drücke auf Kegelförmige Spitzen bei Bewegung mit Uberschallgeschwindigkeit", (translation) "Pressures on Cone Shaped Tips Moving at Supersonic Velocity", translated by Jack Latsoff, Cornell Aeronautics Library.

4. Taylor, G. I., and Maccoll, J. W., "The Air Pressure on a Cone Moving at High Speeds", Proc. Royal Society, A, p. 139-278, 1933.

5. Puckett, Allen E., and Schamberg, Richard, "Final Report - Galcit Supersonic Wind Tunnel Tests", Library of Aeronautics, California Institute of Technology, June, 1946.

SAMPLE CALCULATIONS

A. Determination of M

Data:

z	P_o	P_A	P_4	P_A	P_s	P_4	Baro
5/8"	102.6	99.2	132.65	70.35	63.30	5.84	74.70

P_o	102.6		P_4	132.65	
P_A	99.2		P_A	70.35	
	3.4			62.30	
Baro	74.7		Baro	74.70	
	3.4			62.30	
P_o	= 71.3		P_4	= 12.40	

$$\frac{P_4}{P_o} = \frac{12.4}{71.3} = .1739$$

$$\frac{.2188\ (P_4 - P_s)}{P_o} = \frac{.2188\ (58.4 - 63.3)}{71.3} = -.01504$$

$$\frac{P_s}{P_o} = .1739 - .0150 = .1575$$

$$M = 1.860$$

B. Determination of Angle of Attack

Data:

	Rel. Angle	P_S	P_A	ΔP
Hole up	0	112.70	92.10	20.60
Hole up	1.0	112.90	91.85	21.05
Hole down	0	112.90	91.85	21.05
Hole down	1.0	112.65	92.15	20.50

C. Determination of P_s/P_o; M = 1.86

Data:

Run	Model	P_o	P_A	Baro	P_s	P_A	P_4	P_A	T
52	3	102.65	99.15	74.88	121.6	81.6	75.45	13.35	23.3

P_o	102.65	P_s	121.6
P_A	99.15	P_A	81.8
	3.50		39.8
Baro	74.88	Baro	74.88
	3.50		39.8
P_o =	71.38	P_s =	35.08

$$P_s/P_o = \frac{35.08}{71.38} = .4915$$

D. Determination of P_s/P_o'; M = 1.86

$$\frac{P_o}{P_o'} = \left(\frac{2.8}{2.4} M^2 \sin^2\theta_w - \frac{.4}{2.4}\right)^{2.5} \left(\frac{.2\ M^2 \sin^2\theta_w + 1}{1.2\ M^2 \sin^2\theta_w}\right)^{3.5}$$

$$= \left(\frac{2.8}{2.4} (1.86)^2(\sin 58.2)^2 - \frac{.4}{2.4}\right)^{2.5} \left(\frac{.2(1.86)^2(\sin 58.2)^2+1}{1.2(1.86)^2(\sin^2 58.2)^2}\right)^{3.5}$$

$$= 1.108$$

$$\frac{P_s}{P_o'} = \frac{P_s}{P_o'} \times \frac{P_o}{P_o'} = .491 \times 1.108 = .544$$

E. Determination of M = 1 on cone

$$\left(\frac{P_s}{P_o}\right)_{M=1} = .528 \frac{P_o'}{P_o} = \frac{.528}{1.108} = .477$$

F. Determination of P_s/P_o (Kopal theoretical)

$$\frac{P_s}{P_o} = \frac{P_s}{P_w} \times \frac{P_w}{P_1} \times \frac{P_1}{P_o}$$

$$\frac{P_s}{P_o} = 1.1475 \times 2.74 \times 1.58 = .497$$

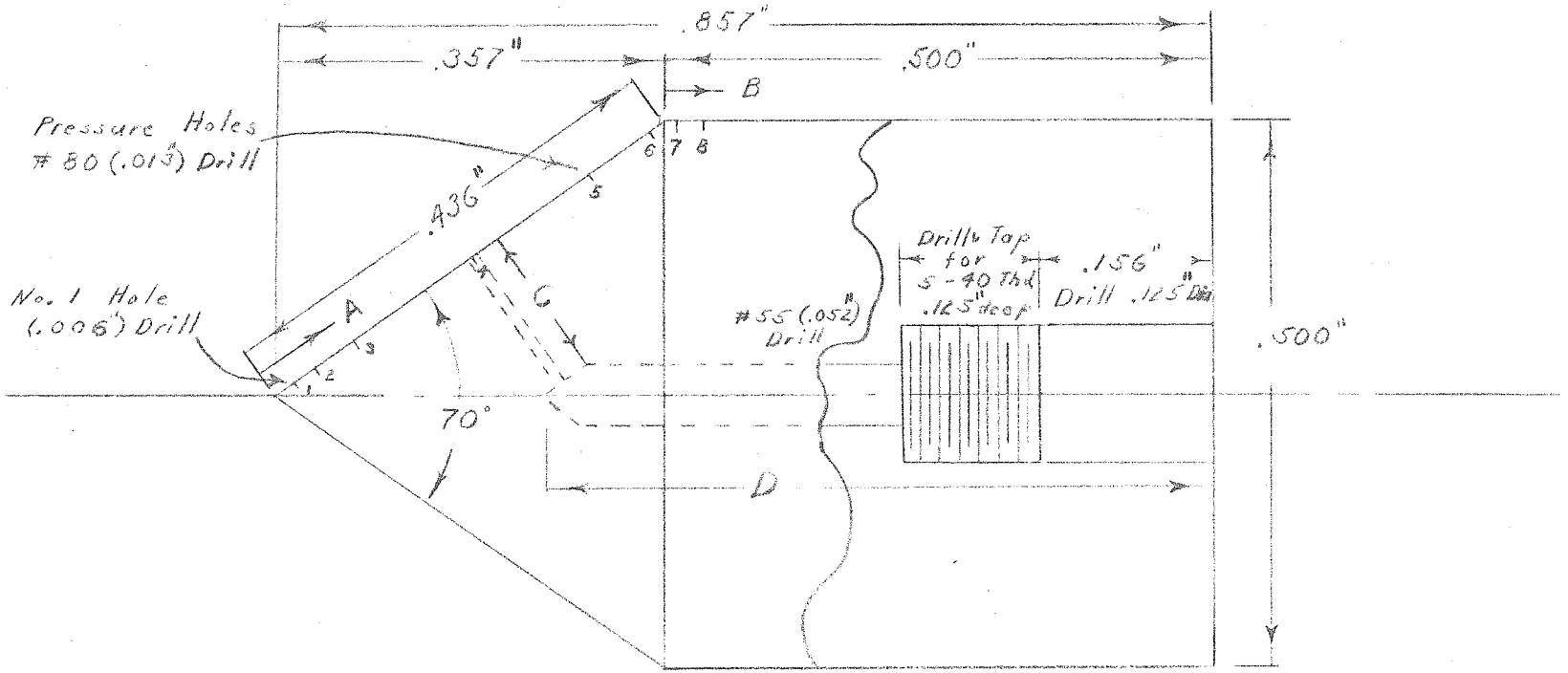

Scale 6" = 1"

Cone #	A	B	C	D
1	.019"		.014"	.840"
2	.044"		.031"	.803"
3	.088"		.061"	.751"
4	.218"		.153"	.591"
5	.350"		.245"	.431"
6	.425"		.299"	.337"
7		.0114"	.255"	.987"
8		.0355"	.243"	.964"

Fig. 1
Cone Pressure
Models

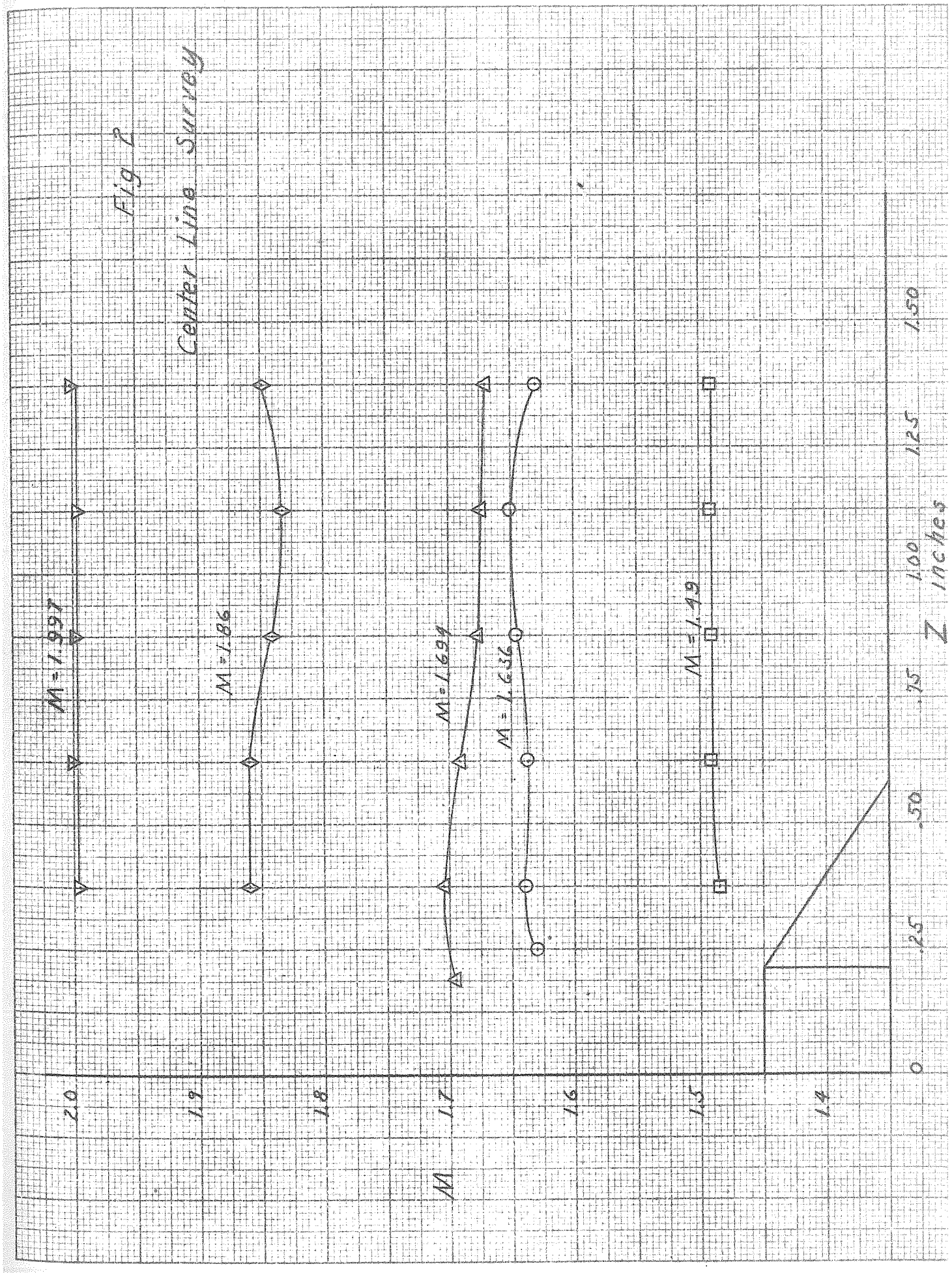
Fig 12
Center Line Survey
M = 1.997
M = 1.86
M = 1.699
M = 1.636
M = 1.49
M
20
19
18
17
16
15
14
0
.25
.50
.75
1.00
1.25
1.50
Z inches

Fig 3 Determination of Angle of Attack

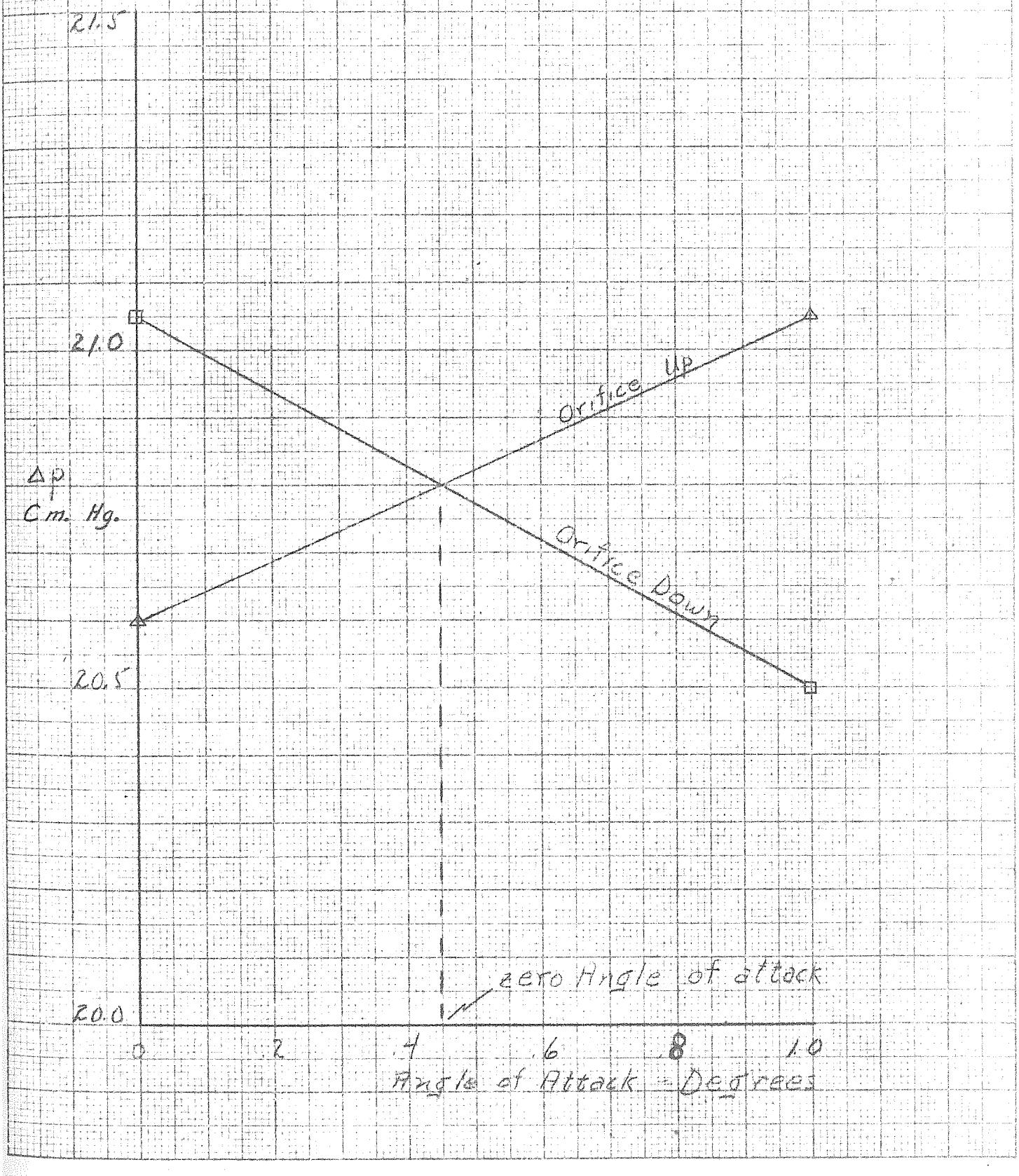

Fig. 4 Symbols

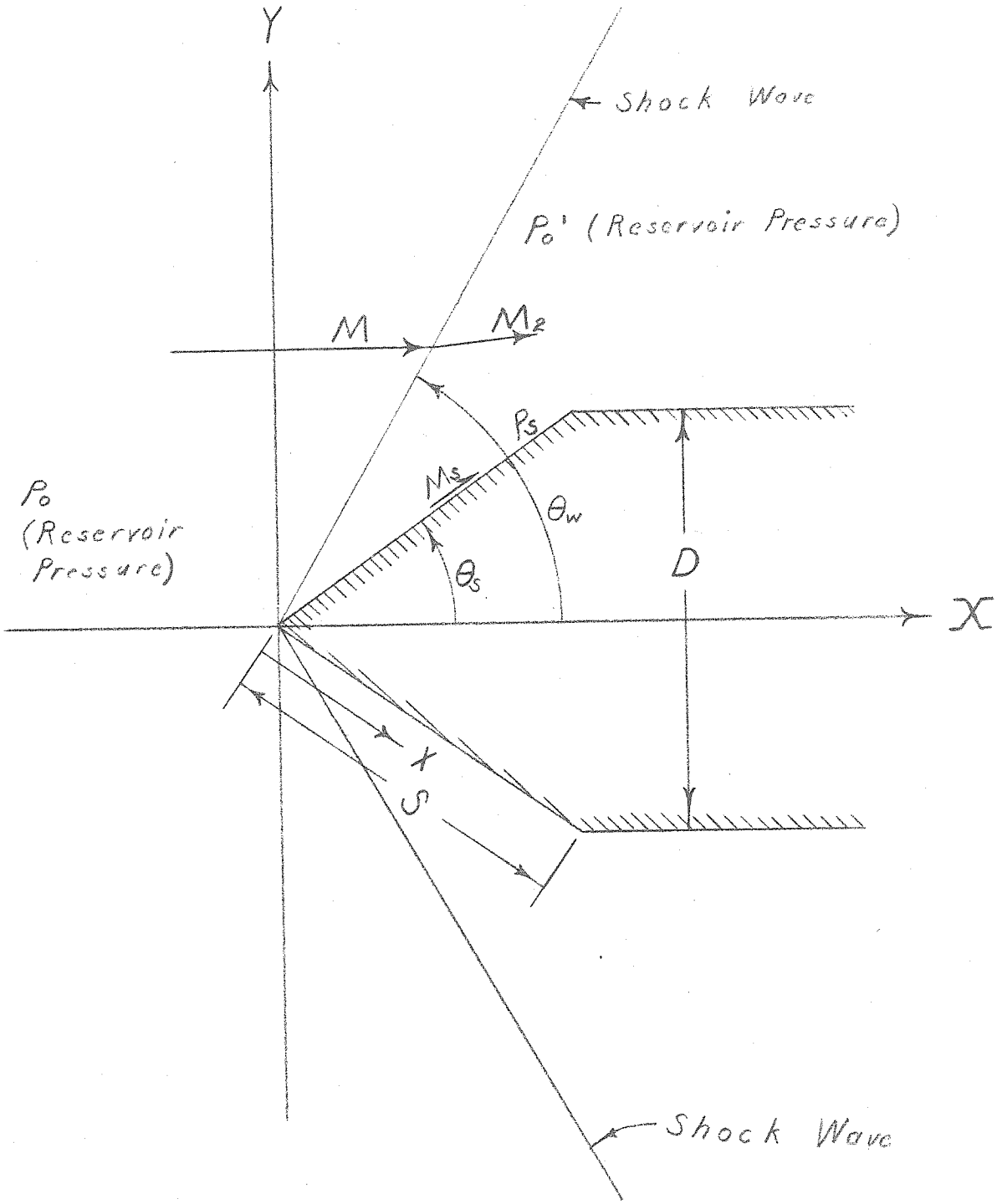

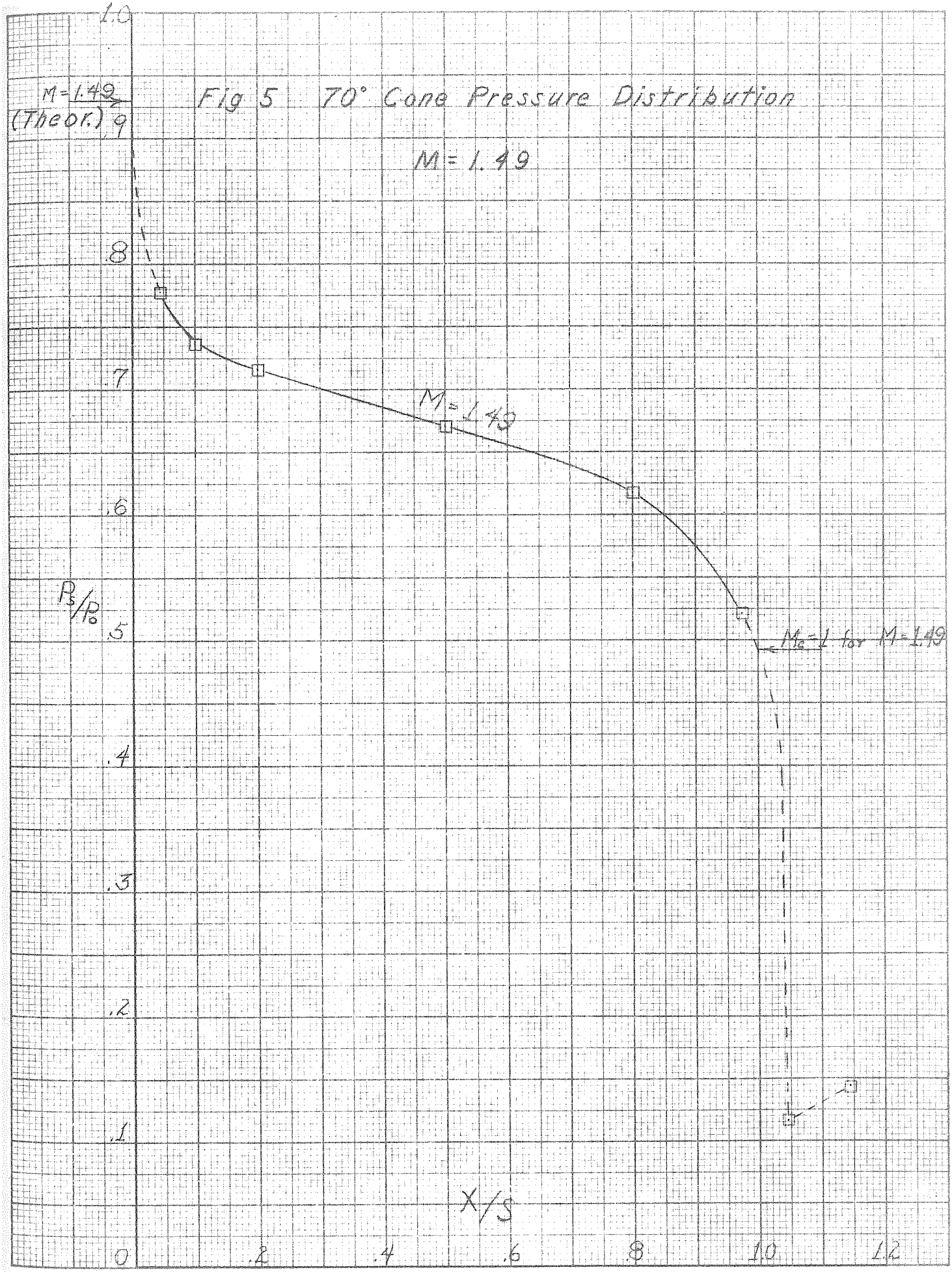
Fig 5 70° Cone Pressure Distribution
M = 1.49
M = 1.49 (Theor.)
M = 1.49
M_s = 1 for M = 1.49
P_s/P_o
X/S
1.0
.9
.8
.7
.6
.5
.4
.3
.2
.1
0
.2
.4
.6
.8
1.0
1.2

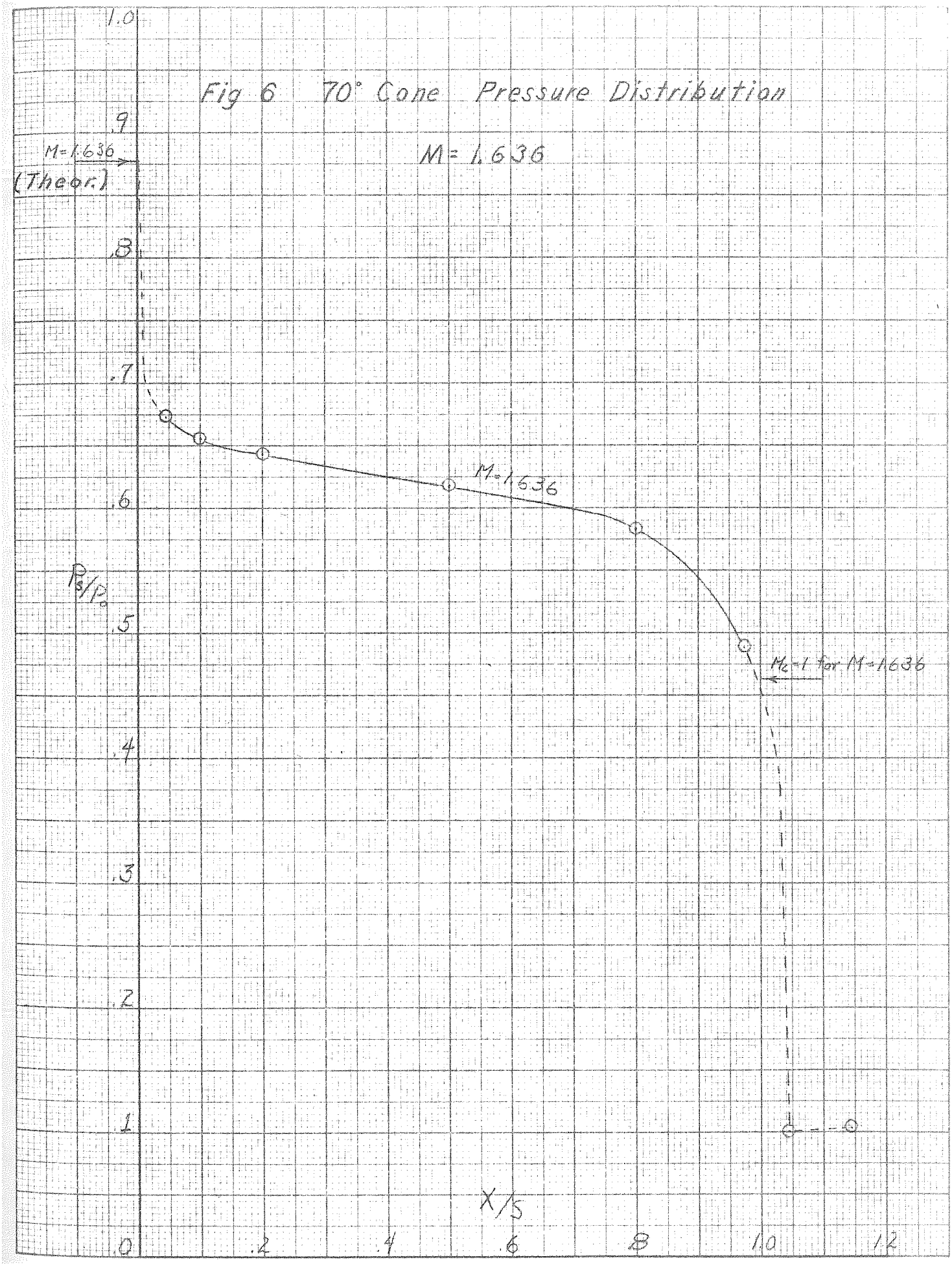
Fig 6 70° Cone Pressure Distribution
M = 1.636
M=1.636
(Theor.)
M=1.636
M_2=1 for M=1.636
P_s/P_o
X/5
1.0
.9
.8
.7
.6
.5
.4
.3
.2
.1
.0
.2
.4
.6
.8
1.0
1.2

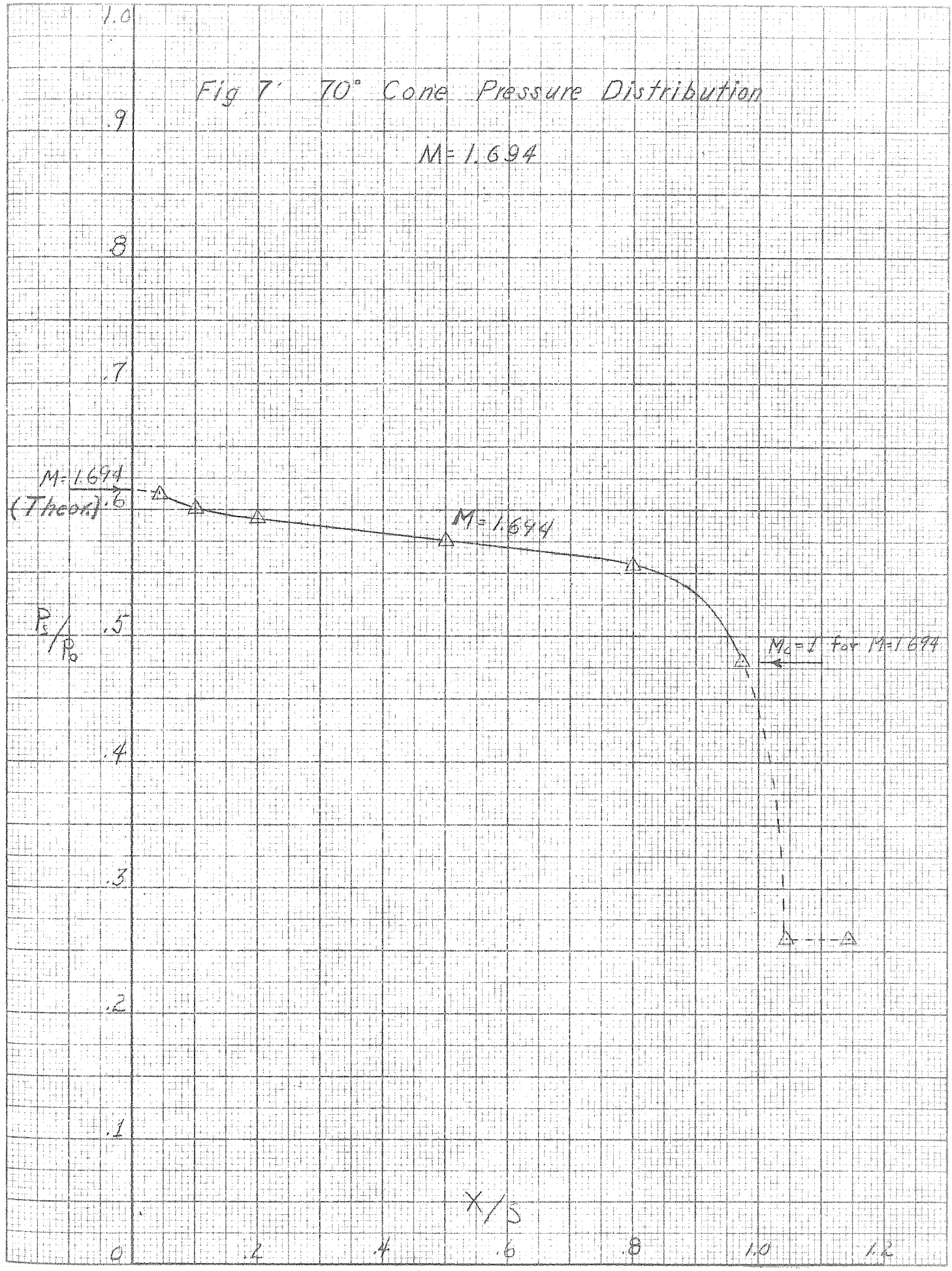
Fig 7' 70° Cone Pressure Distribution
M = 1.694
M = 1.694 (Theor.)
M = 1.694
M∞ = 1 for M = 1.694
Ps/P0
X/S
1.0
.9
.8
.7
.6
.5
.4
.3
.2
.1
0
.2
.4
.6
.8
1.0
1.2

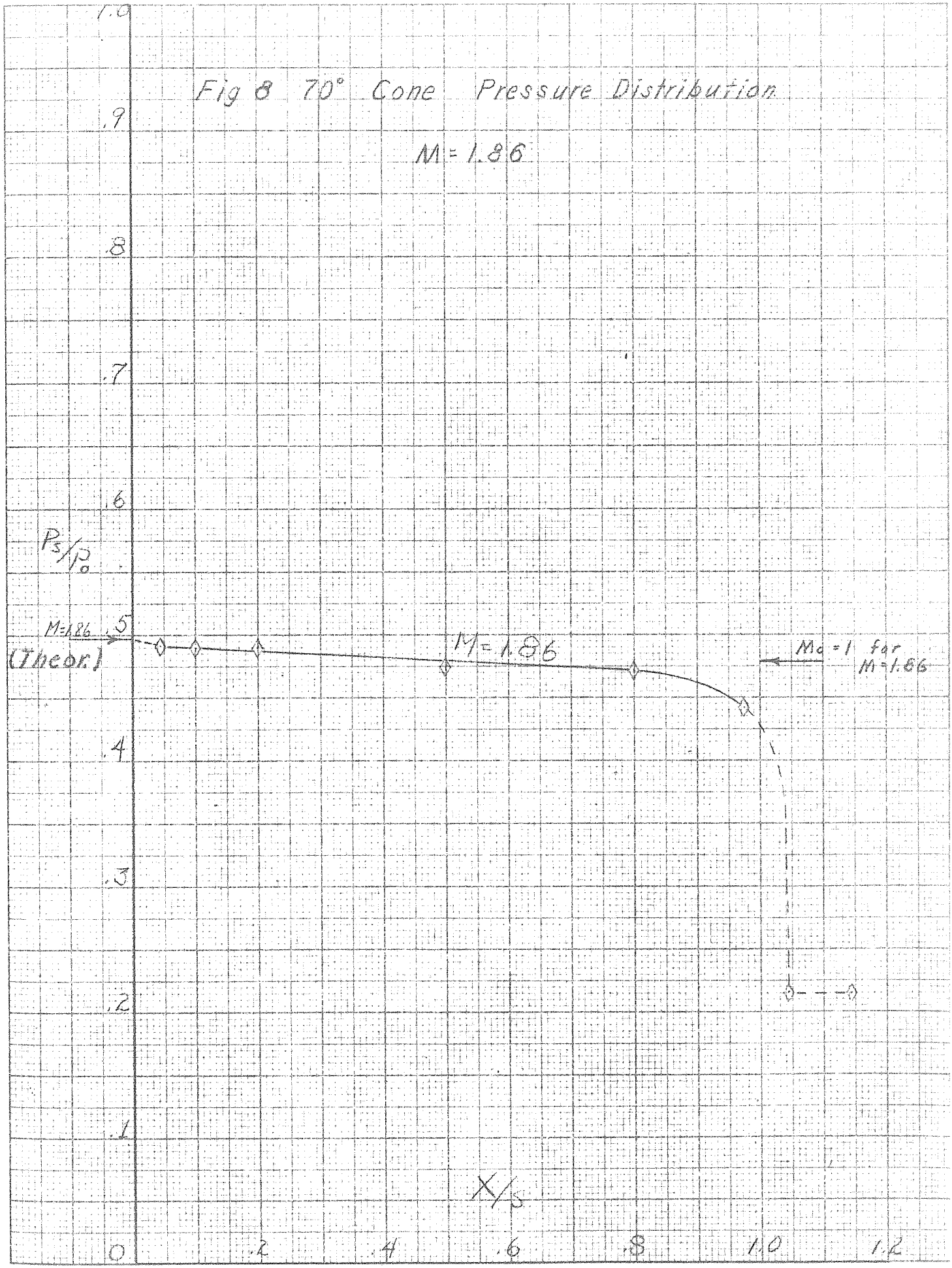
Fig 8 70° Cone Pressure Distribution
M = 1.86
1.0
.9
.8
.7
.6
P_s/P_o
.5
M=1.86 (Theor.)
M = 1.86
M_a = 1 for M = 1.86
.4
.3
.2
.1
0
X/s
.2
.4
.6
.8
1.0
1.2

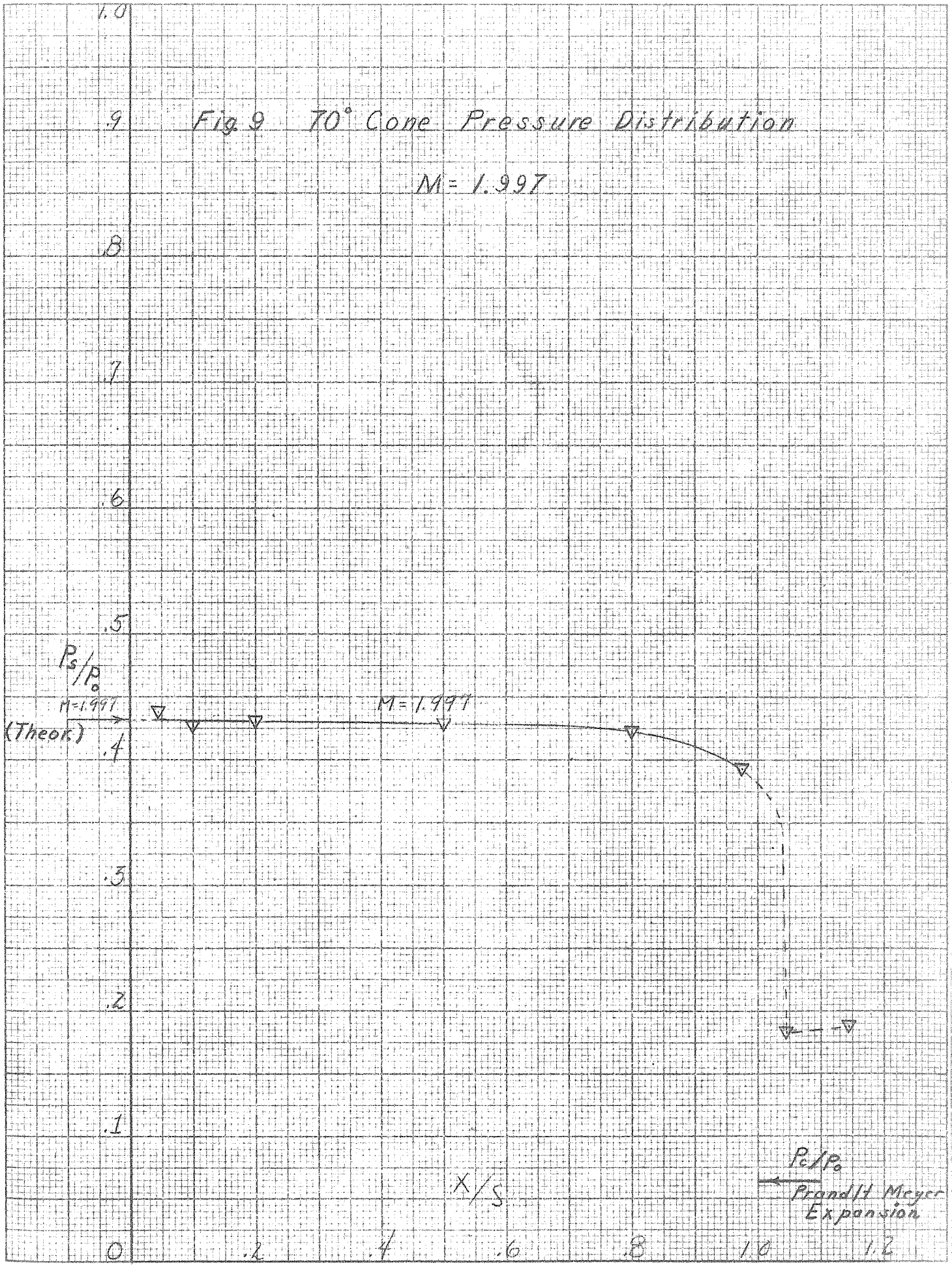
Fig. 9 70° Cone Pressure Distribution
M = 1.997
1.0
.9
.8
.7
.6
.5
.4
.3
.2
.1
0
Ps/Po
M=1.997
(Theor.)
M = 1.997
Pe/Po
Prandtl Meyer
Expansion
X/S
.2
.4
.6
.8
1.0
1.2

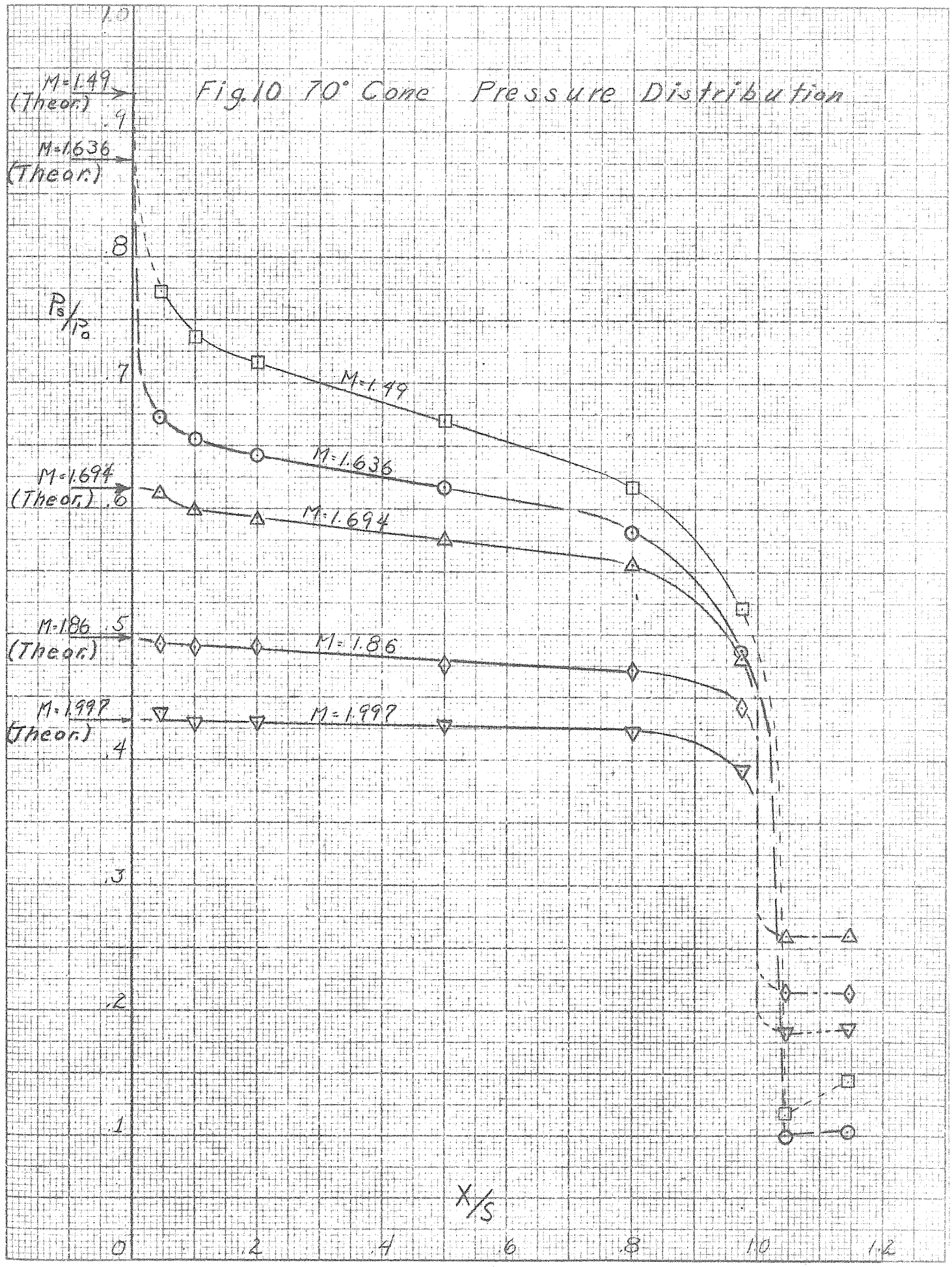
Fig. 10 70° Cone Pressure Distribution
M=1.49 (Theor.)
M=1.636 (Theor.)
M=1.694 (Theor.)
M=1.86 (Theor.)
M=1.997 (Theor.)
M=1.49
M=1.636
M=1.694
M=1.86
M=1.997
Ps/Po
X/S
1.0
.9
.8
.7
.6
.5
.4
.3
.2
.1
0
.2
.4
.6
.8
1.0
1.2

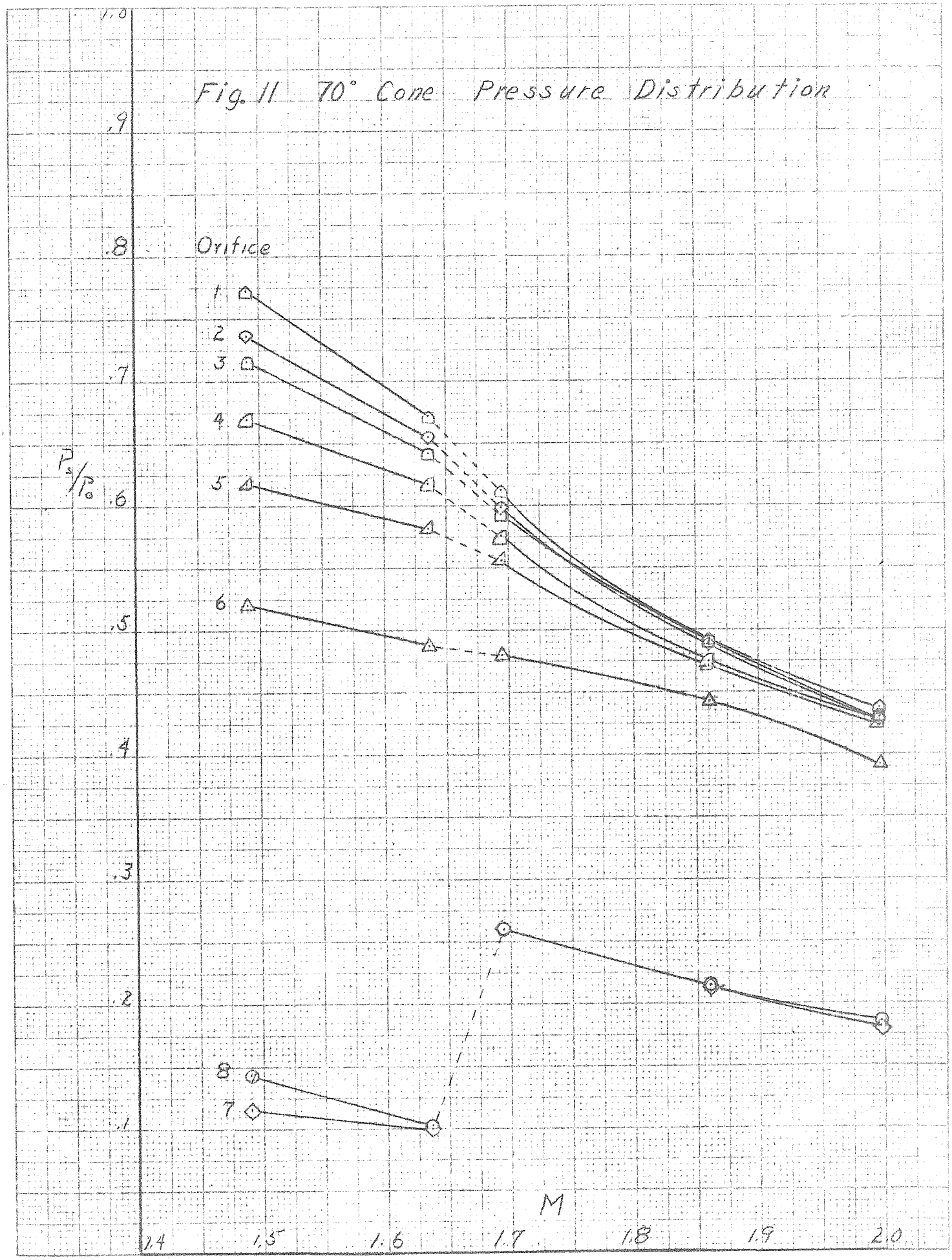
Fig. 11 70° Cone Pressure Distribution
Orifice
1
2
3
4
5
6
7
8
P_s/P_o
1.0
.9
.8
.7
.6
.5
.4
.3
.2
.1
M
1.4
1.5
1.6
1.7
1.8
1.9
2.0

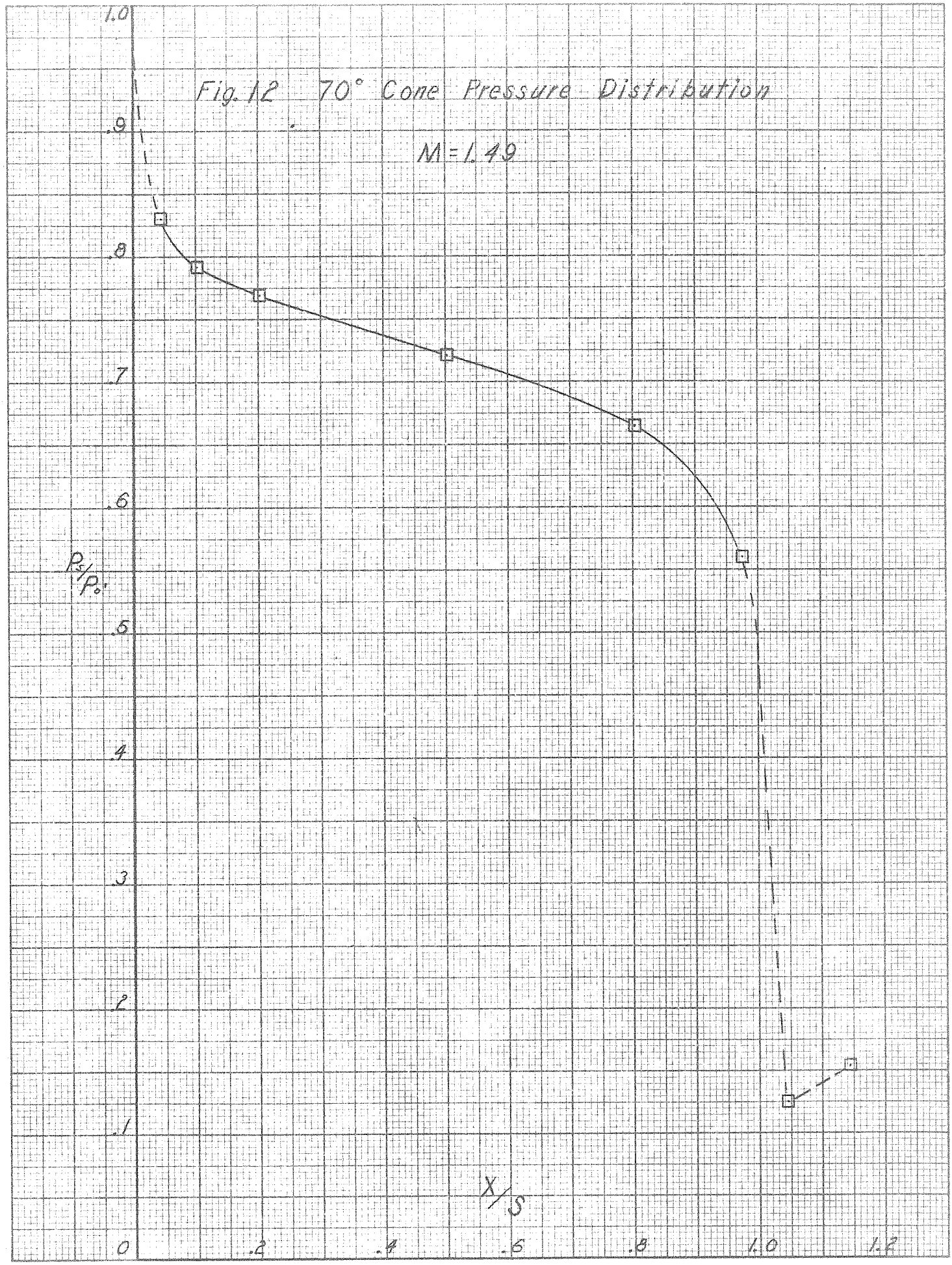
Fig. 12 70° Cone Pressure Distribution
M = 1.49
1.0
.9
.8
.7
.6
.5
.4
.3
.2
.1
0
P_s/P_o
.2
.4
.6
.8
1.0
1.2
X/S

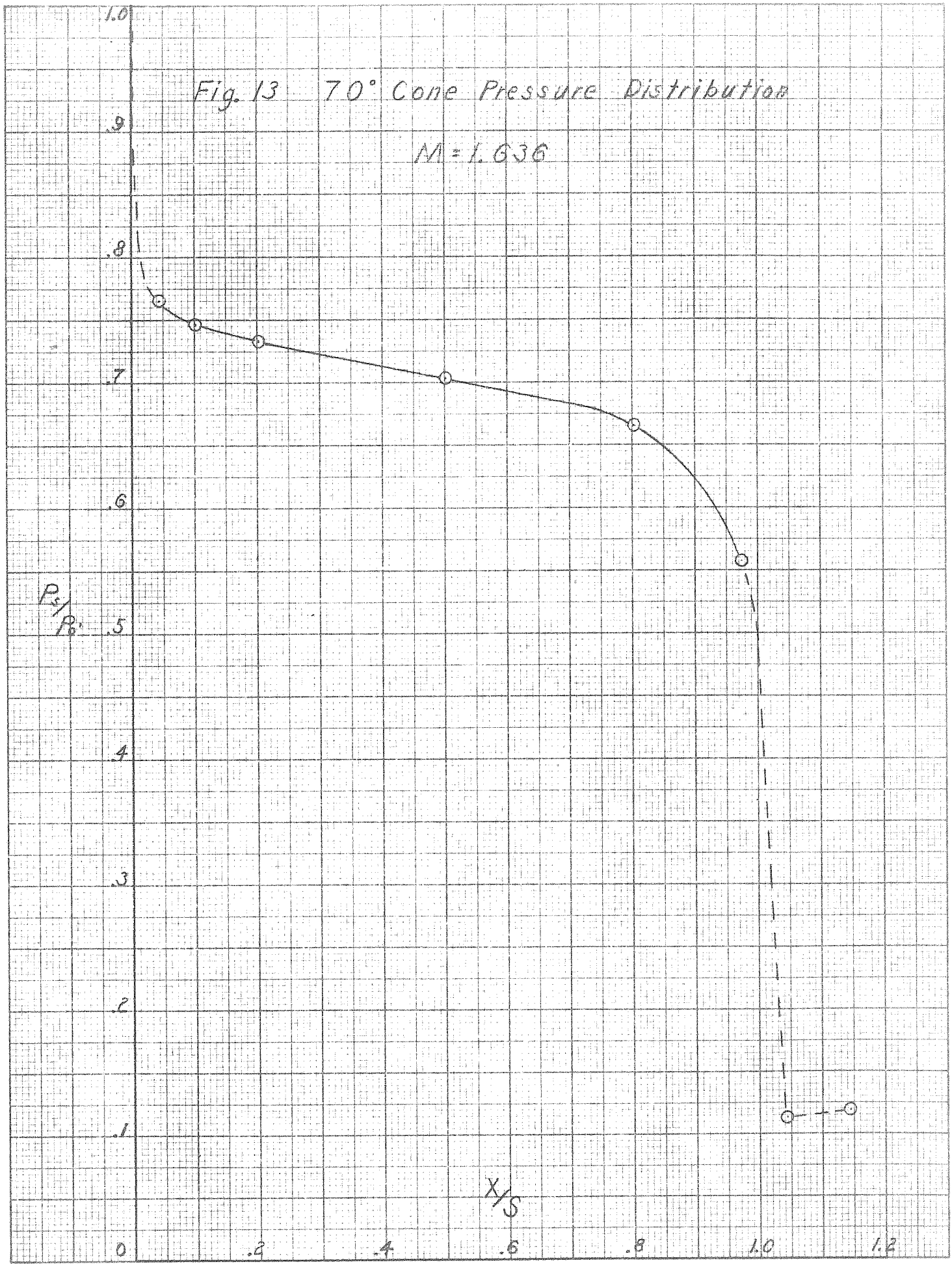
Fig. 13 70° Cone Pressure Distribution
M = 1.636
1.0
.9
.8
.7
.6
.5
.4
.3
.2
.1
0
P_s/P_0
X/S
.2
.4
.6
.8
1.0
1.2

Fig. 14 70° Cone Pressure Distribution

M = 1.694

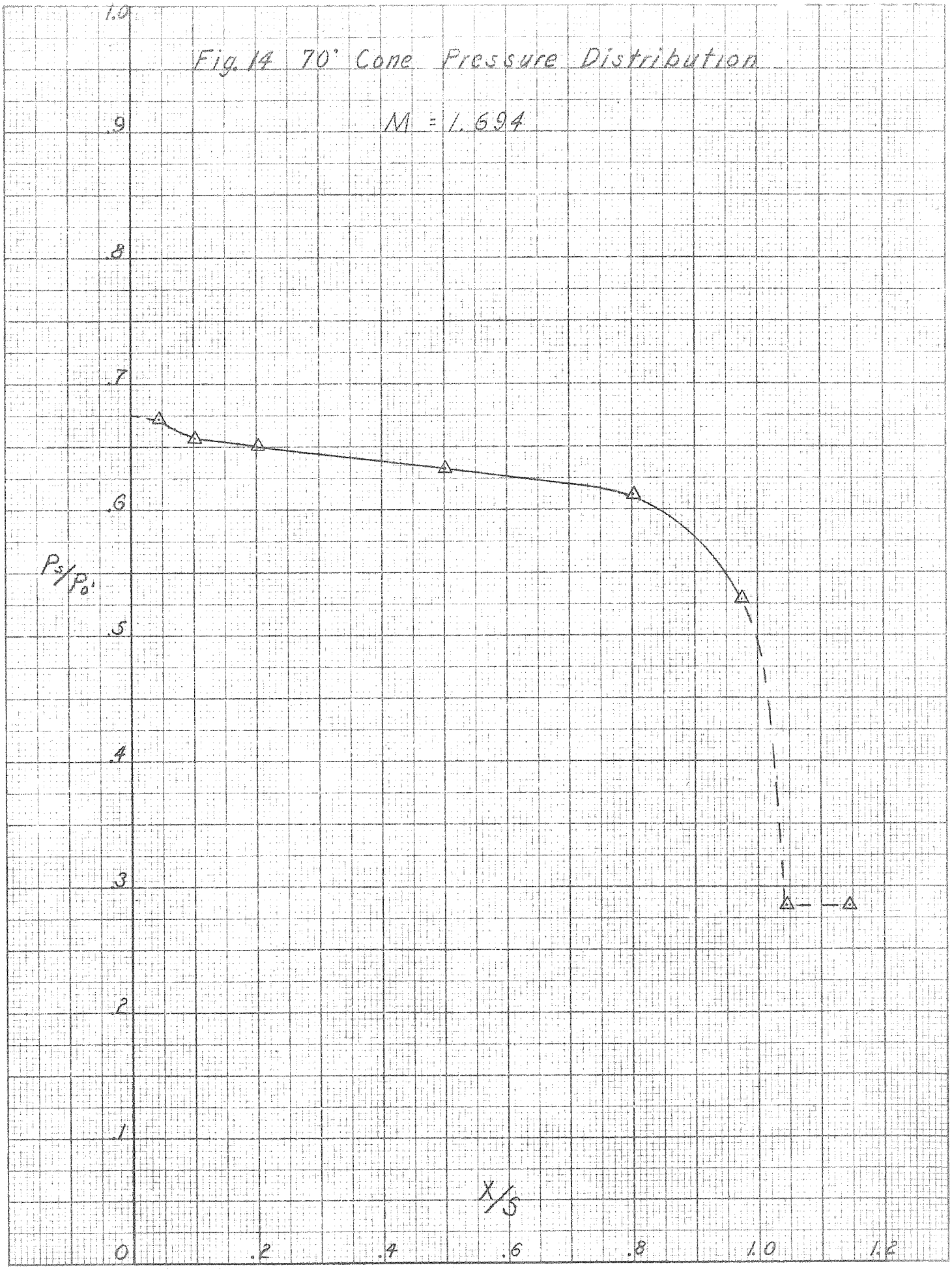

Fig. 15 70° Cone Pressure Distribution

M = 1.86

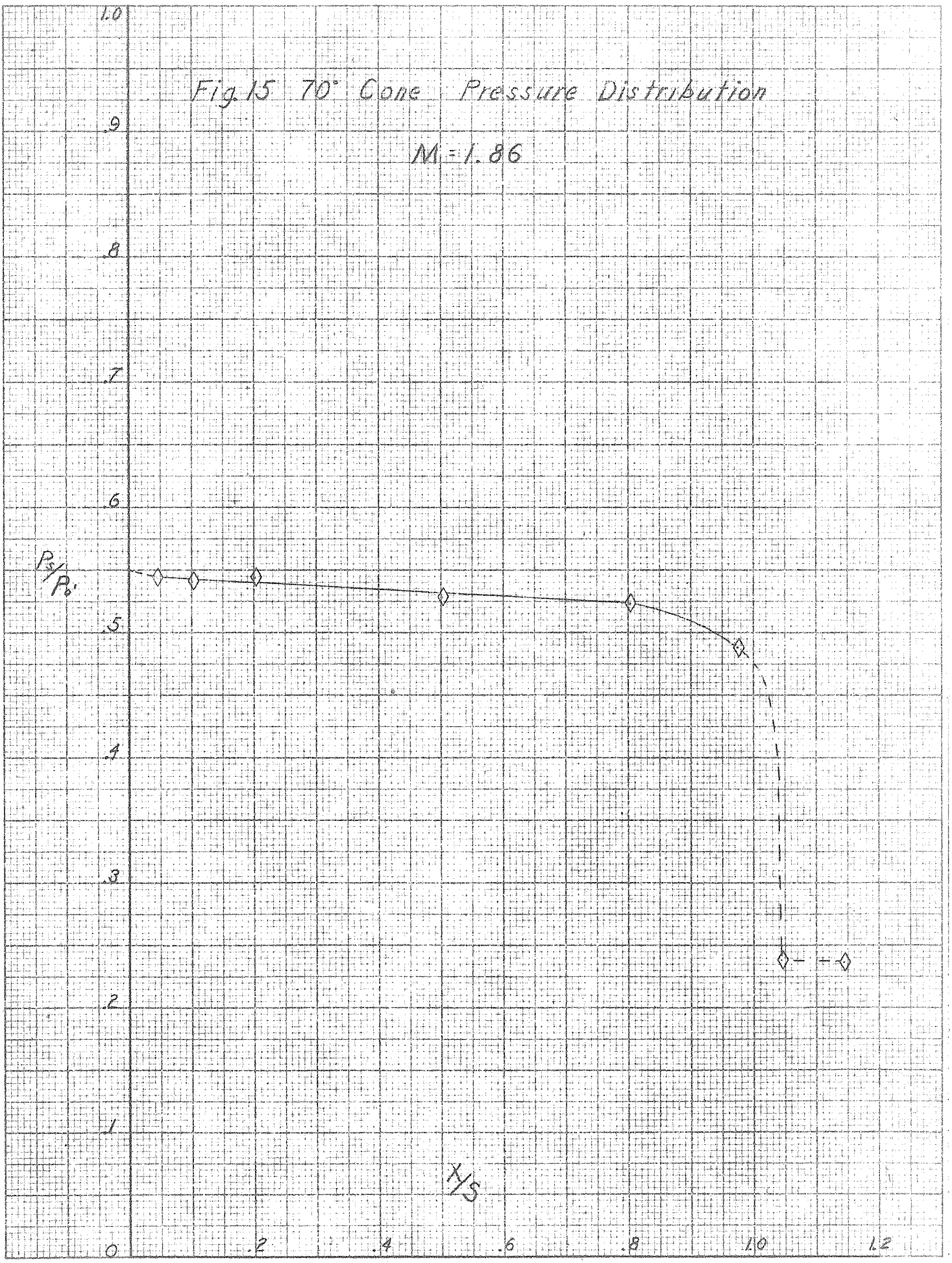

Fig. 16 70° Cone Pressure Distribution

M = 1.997

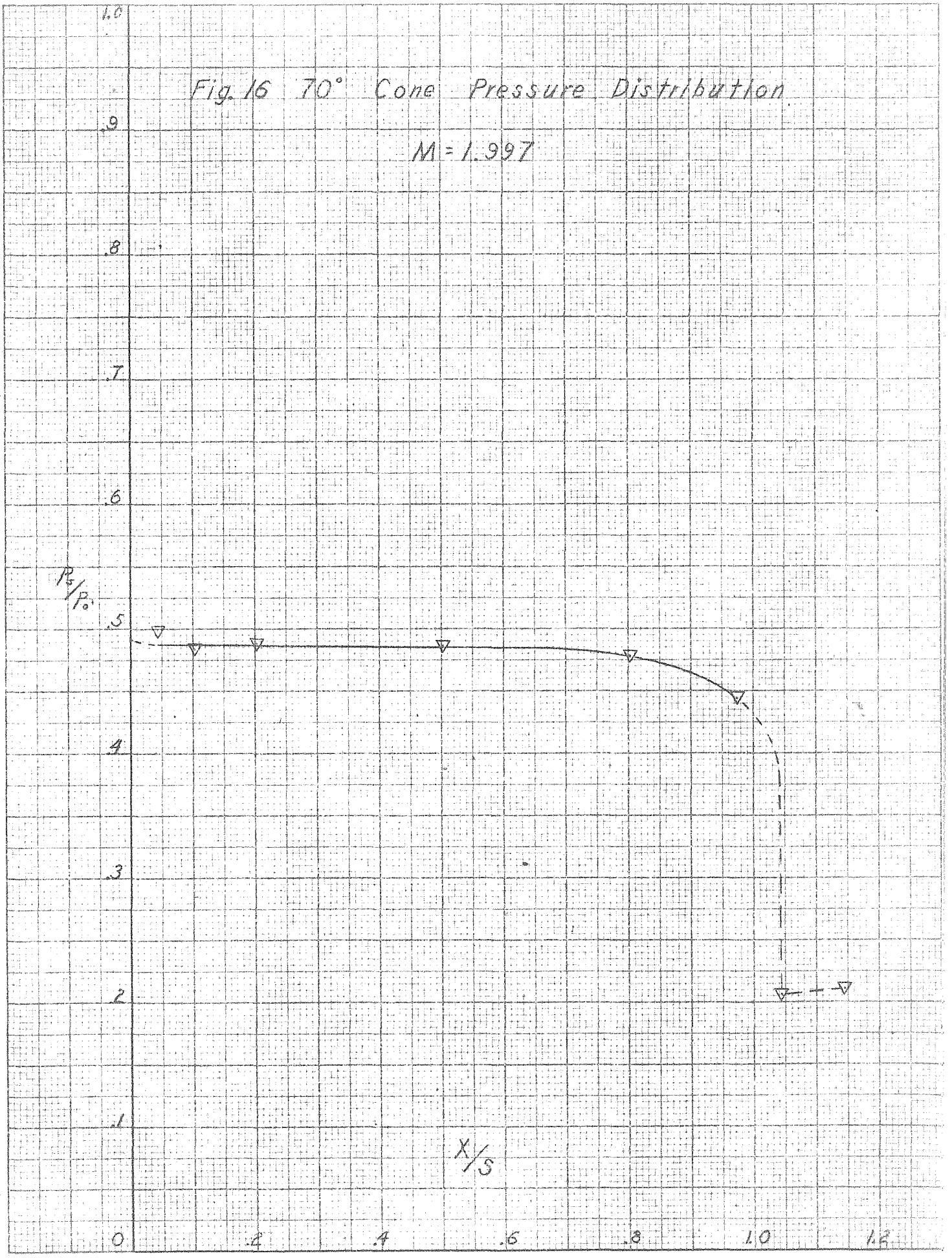

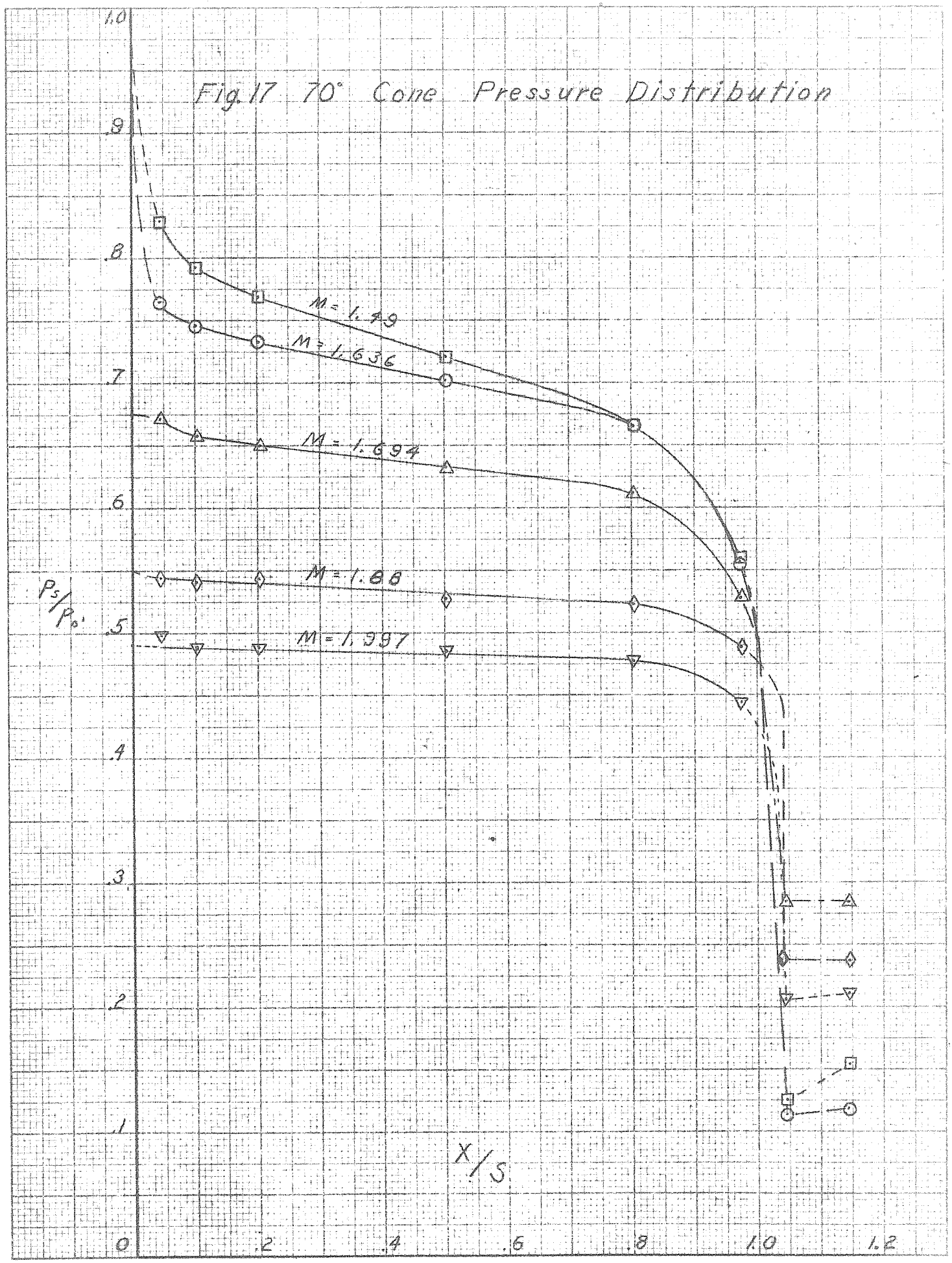
Fig. 17 70° Cone Pressure Distribution
M = 1.79
M = 1.636
M = 1.694
M = 1.88
M = 1.997
P_s/P_o
X/S
1.0
.9
.8
.7
.6
.5
.4
.3
.2
.1
0
.2
.4
.6
.8
1.0
1.2

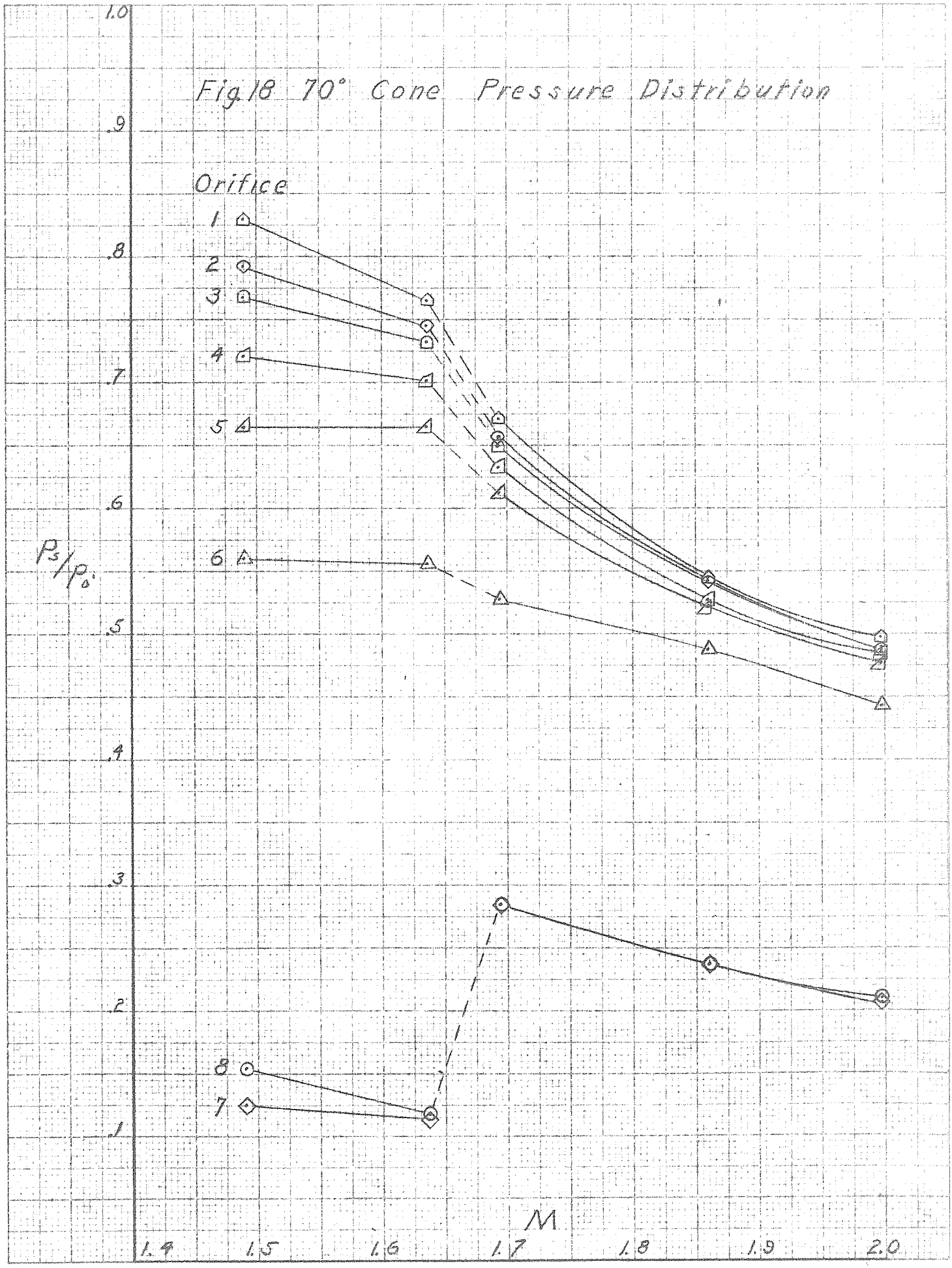
Fig 18 70° Cone Pressure Distribution
Orifice
1
2
3
4
5
6
7
8
P_3/P_0
1.0
.9
.8
.7
.6
.5
.4
.3
.2
.1
M
1.4
1.5
1.6
1.7
1.8
1.9
2.0

Fig. 19 70° Cone Shock Wave Pattern

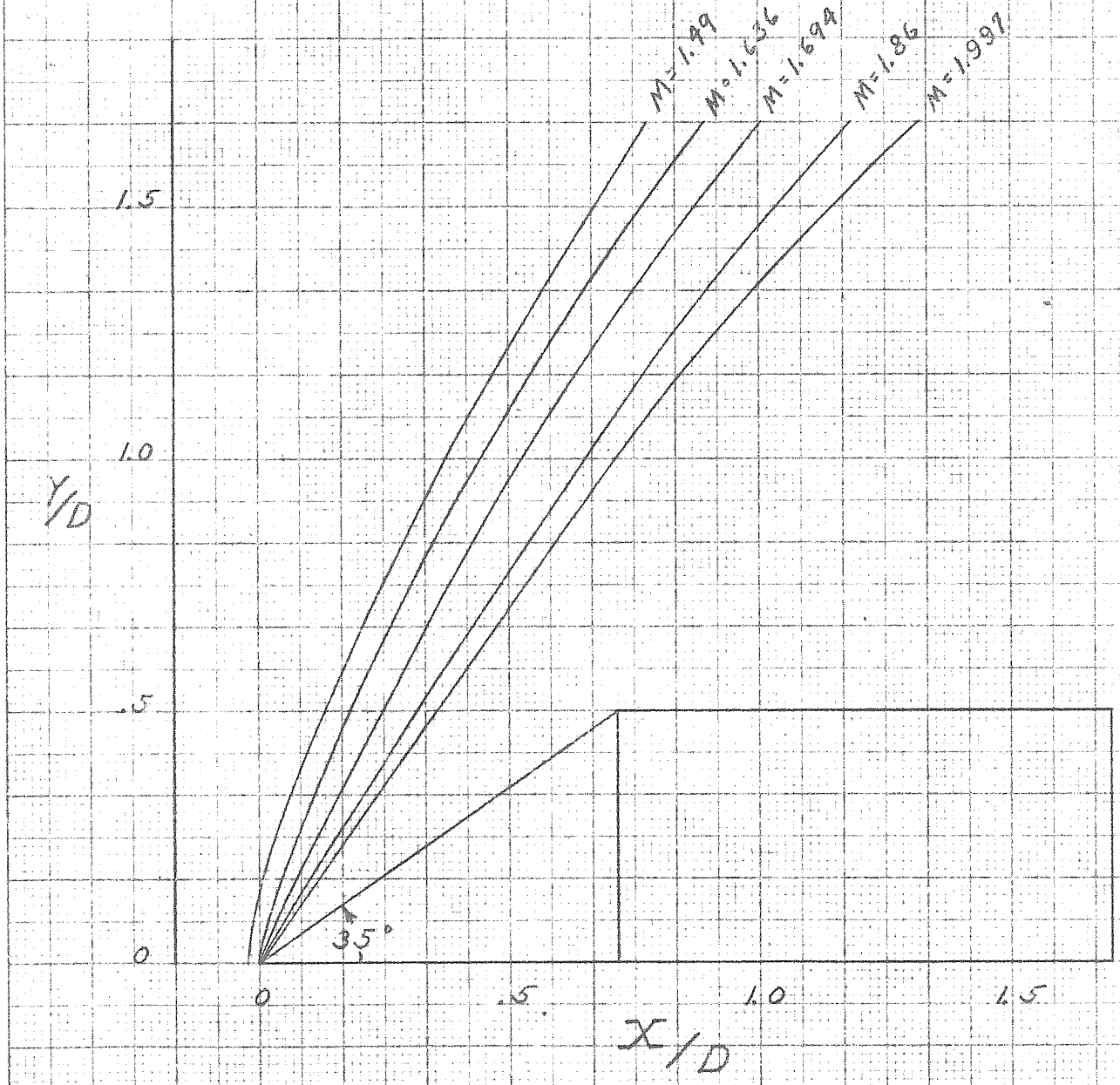

Fig. 20 70° Cone Shock Wave Angle and Mach Number After Shock M = 1.49

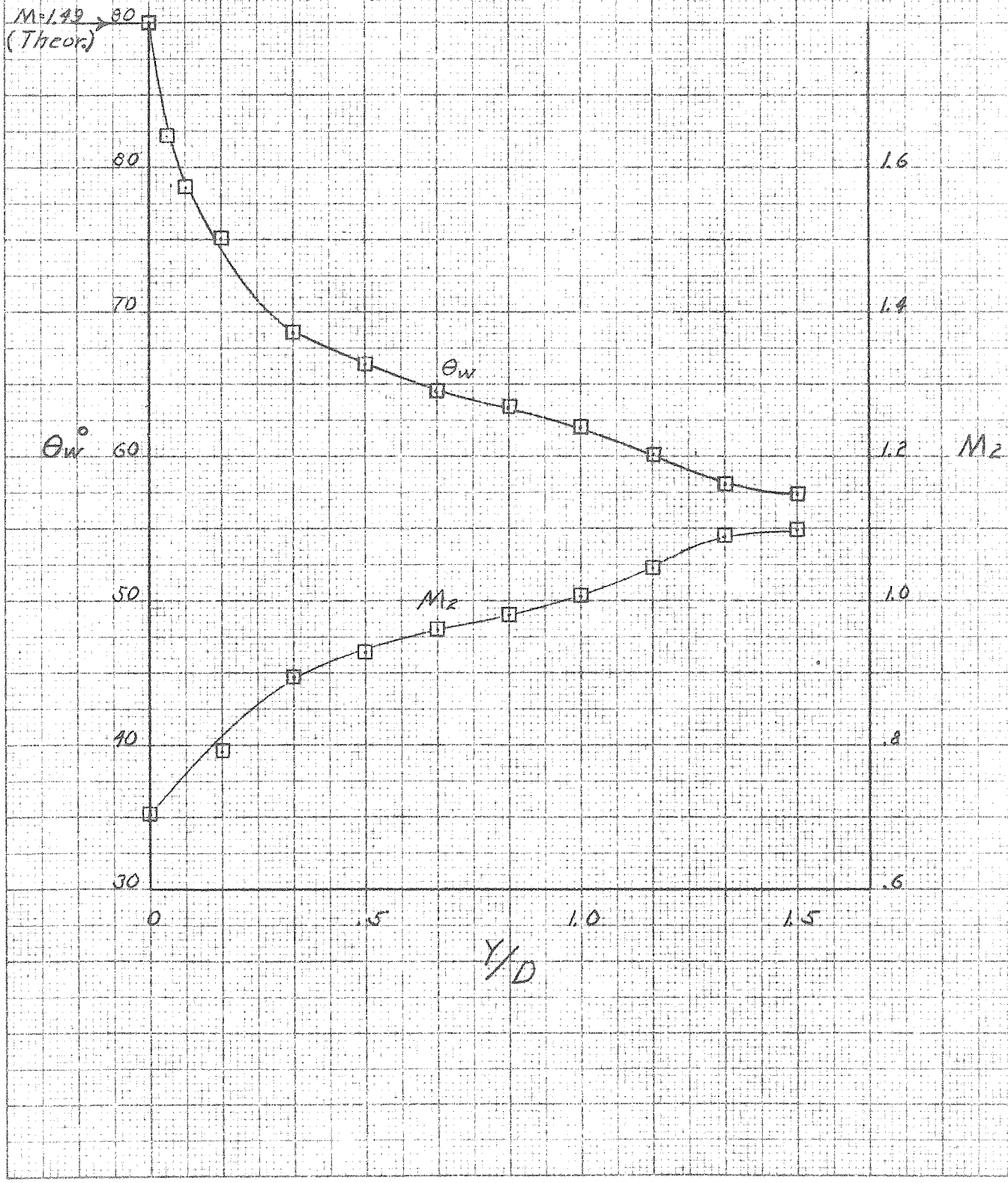

Fig. 21 70° Cone Shock Wave Angle and Mach Number After Shock

M = 1.636

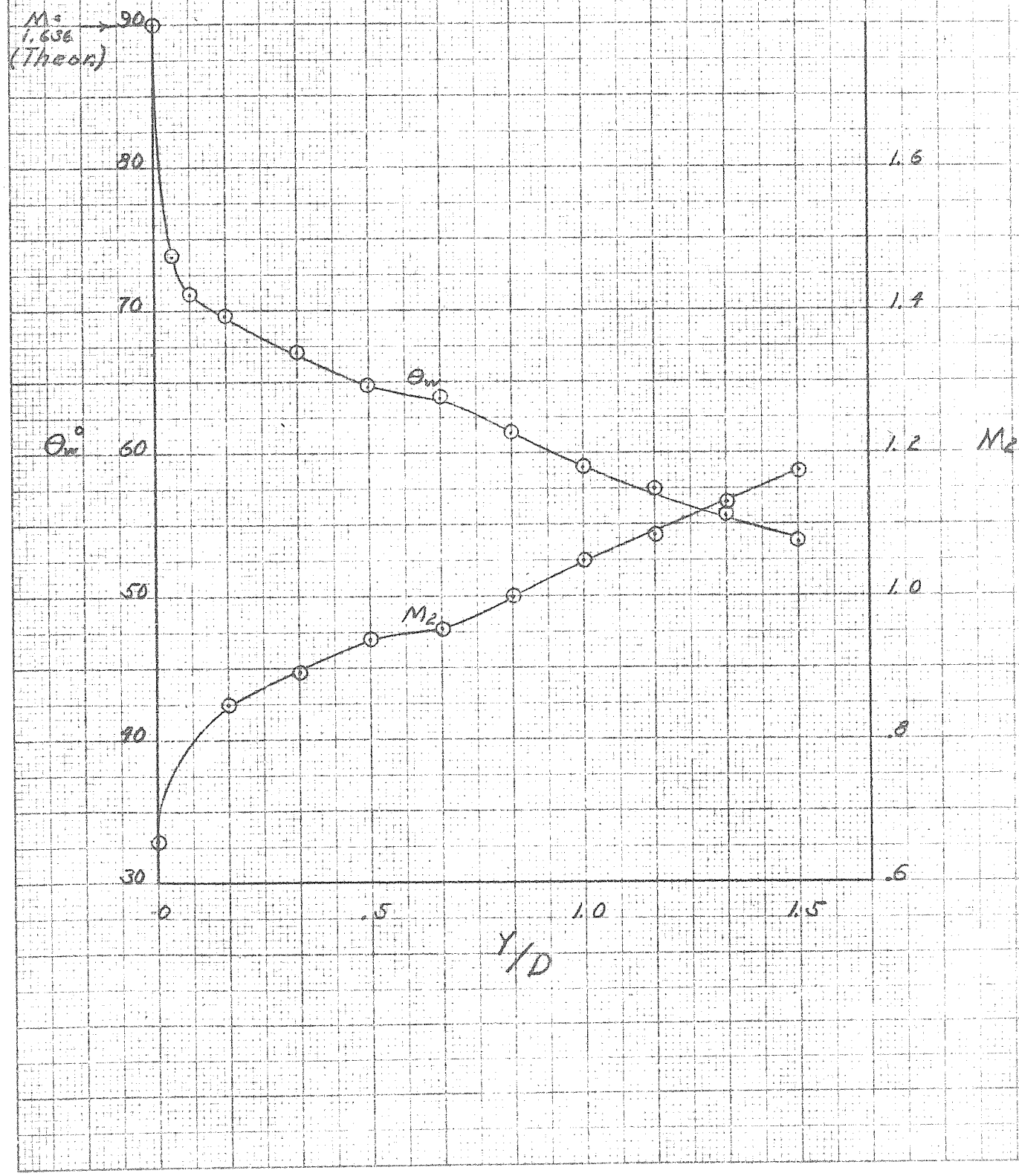

Fig. 22 70° Cone Shock Wave Angle and Mach Number After Shock

M = 1.694

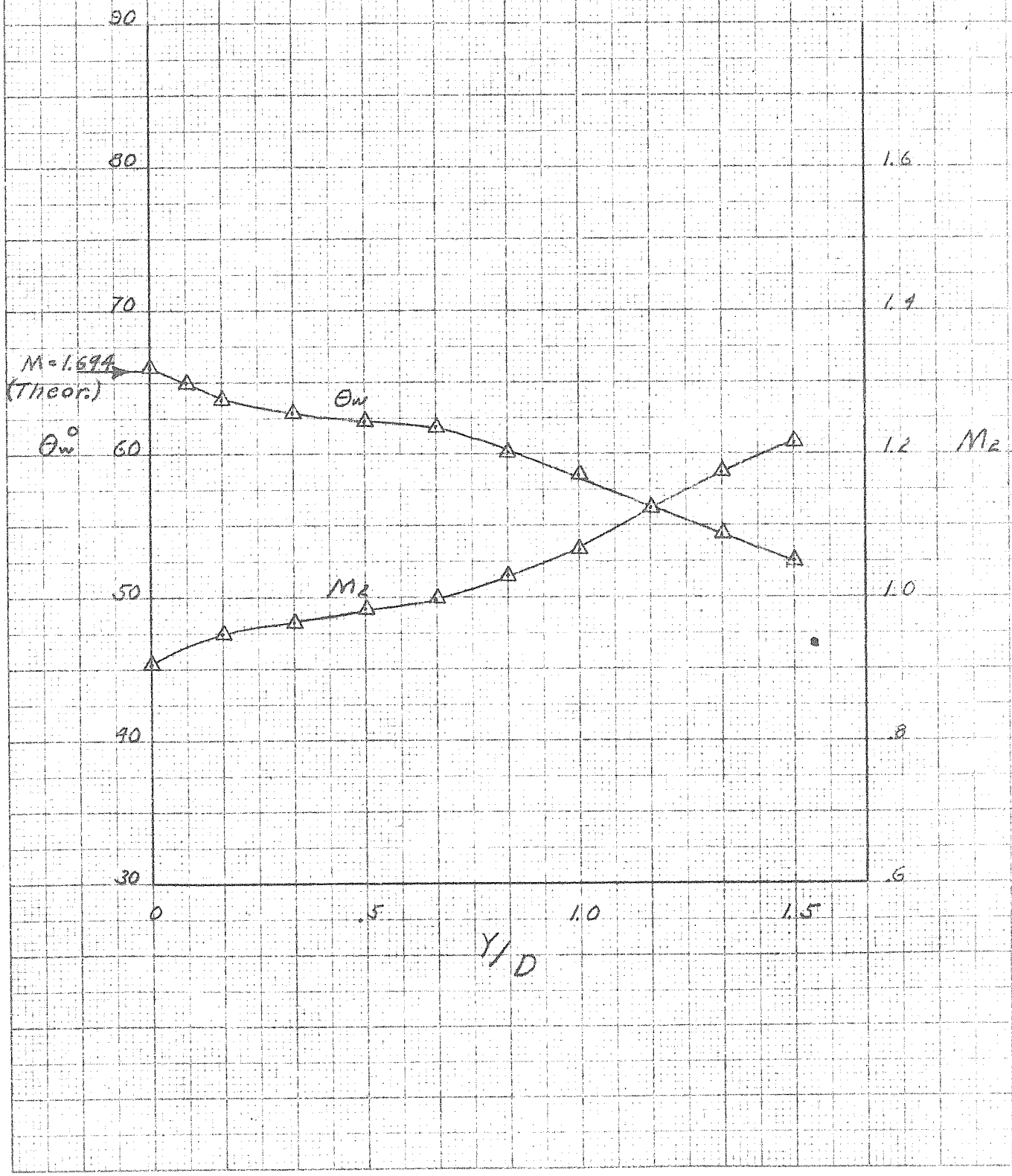

Fig 23 70° Cone Shock Wave Angle and Mach Number After Shock

M = 1.86

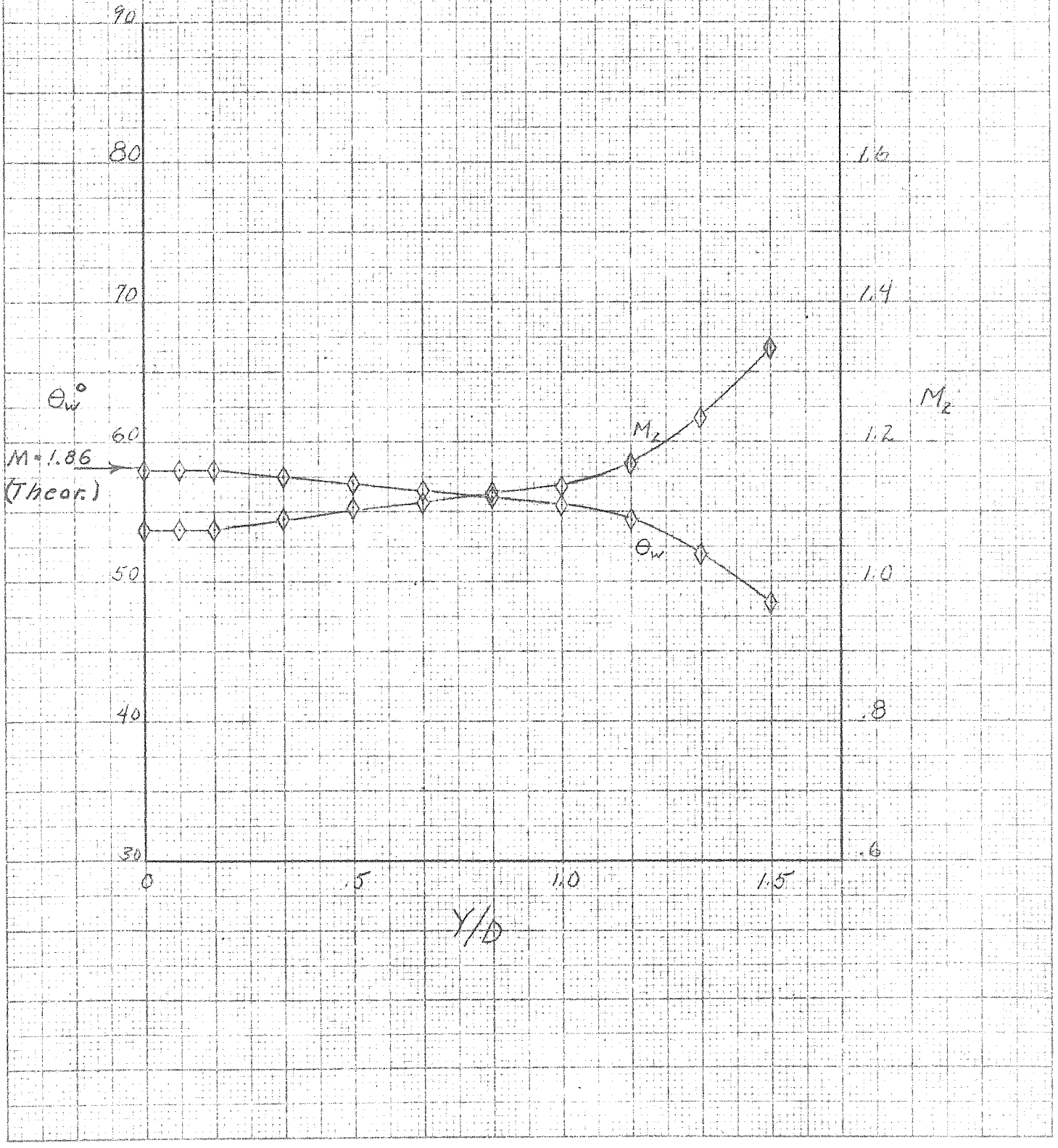

Fig. 24 70° Cone Shock Wave Angle and Mach Number After Shock M = 1.997

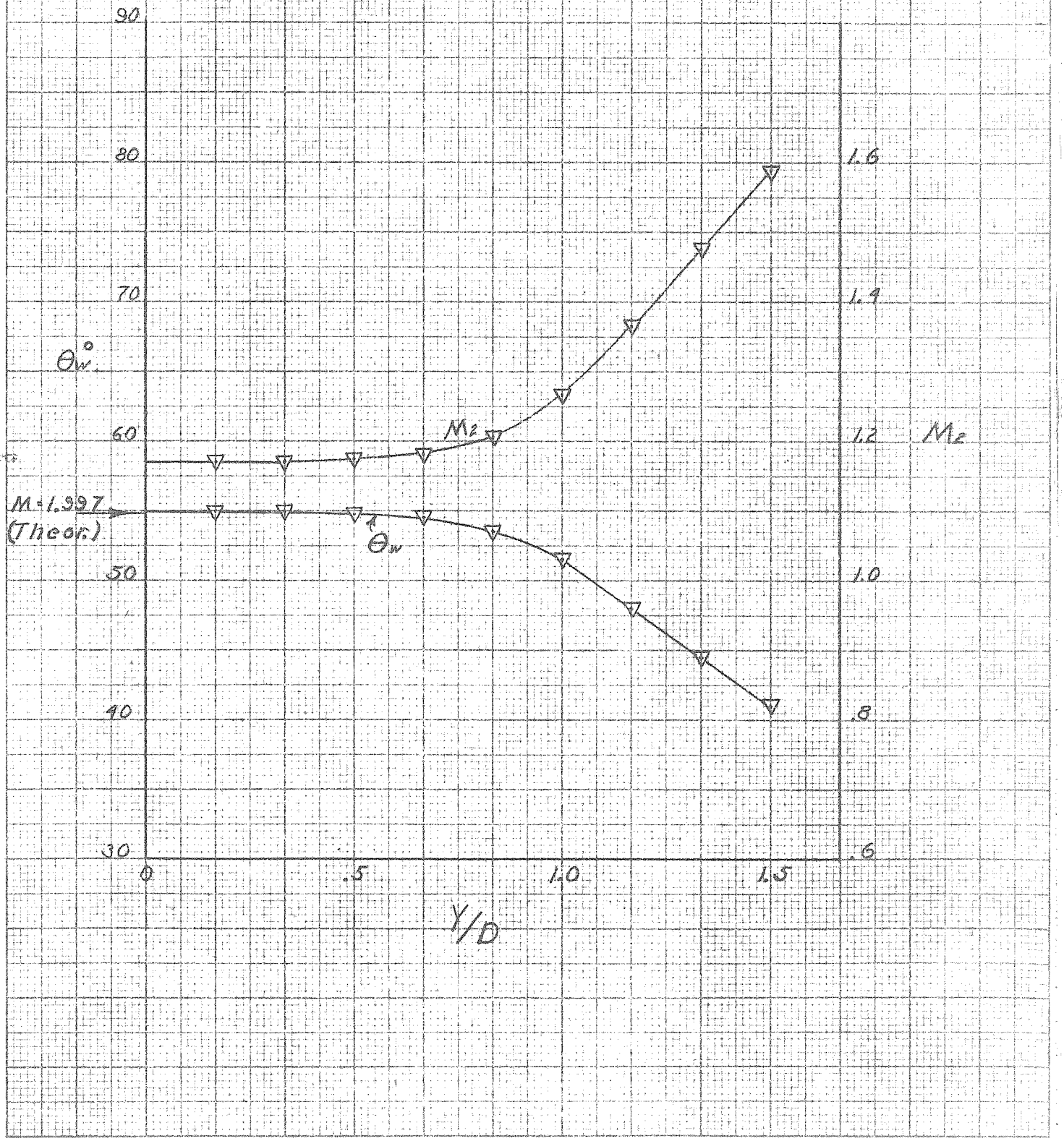

Fig. 25 70° Cone Shock Wave Angle

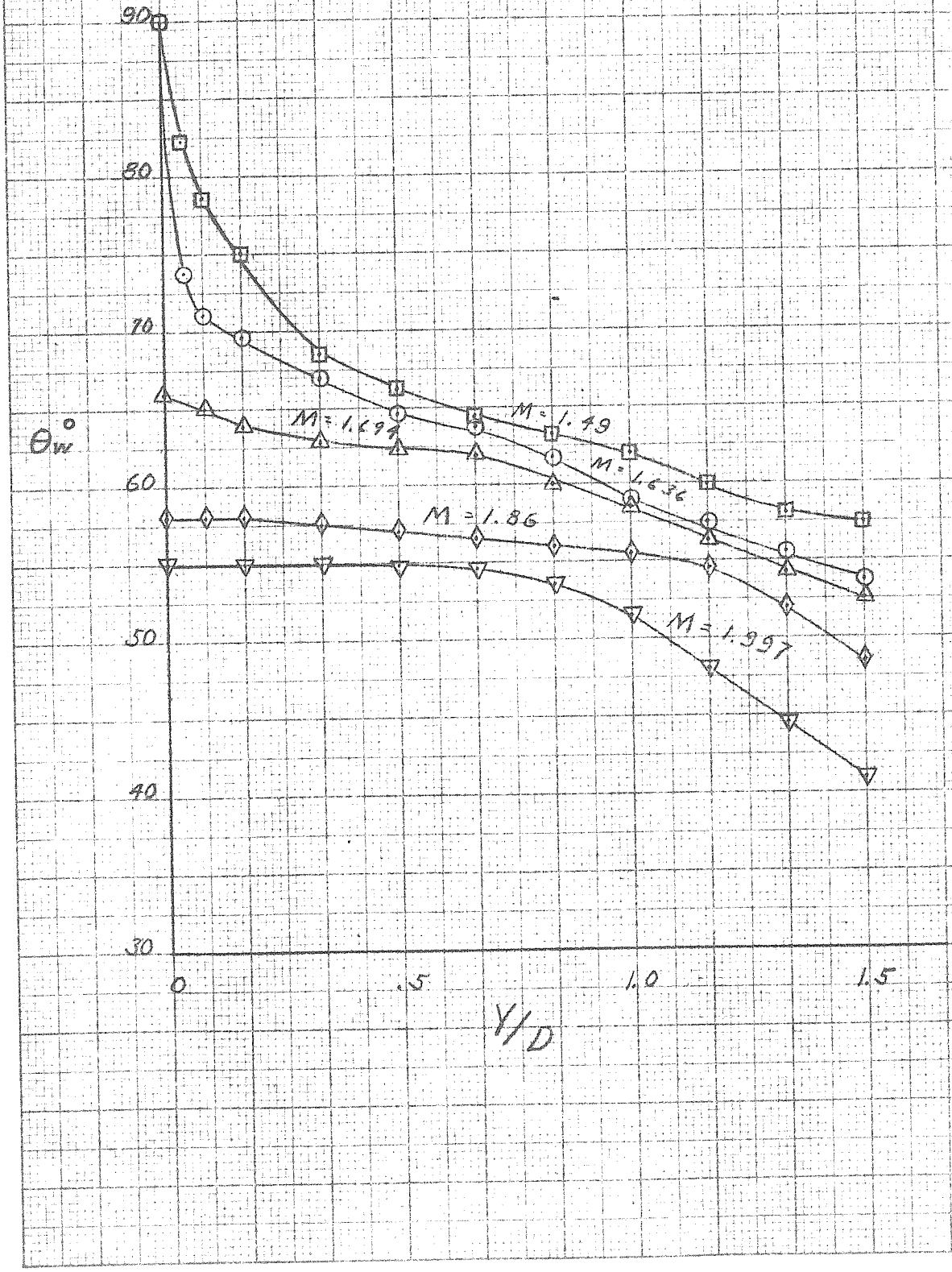

Fig. 26 70° Cone Mach Number Behind Shock

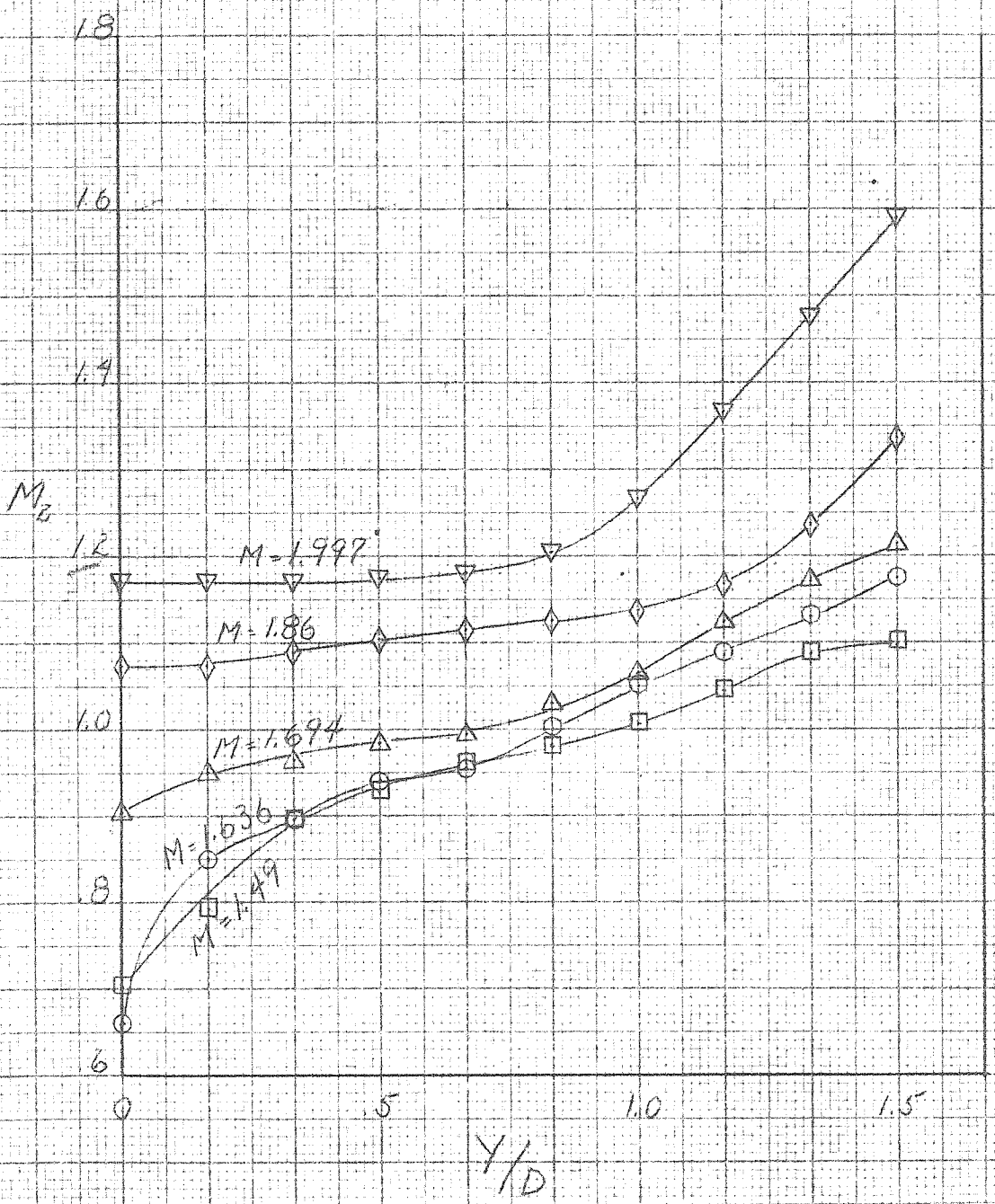

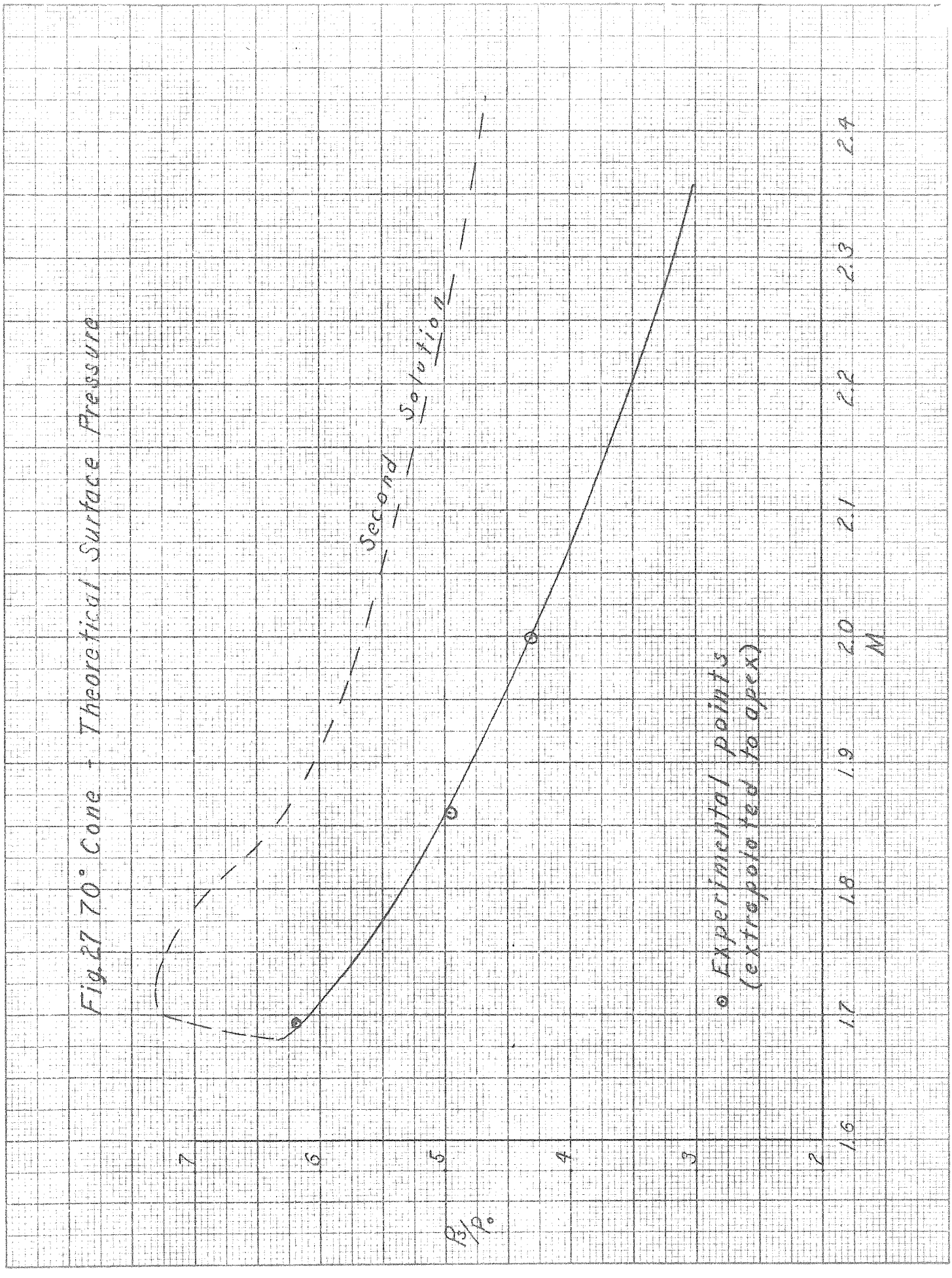
Fig. 27 70° Cone + Theoretical Surface Pressure
Second Solution
o Experimental points
(extrapolated to apex)
p/p0
M
1.6
1.7
1.8
1.9
2.0
2.1
2.2
2.3
2.4
2
3
4
5
6
7

Fig 28 70° Cone Theoretical Shock Wave Angle

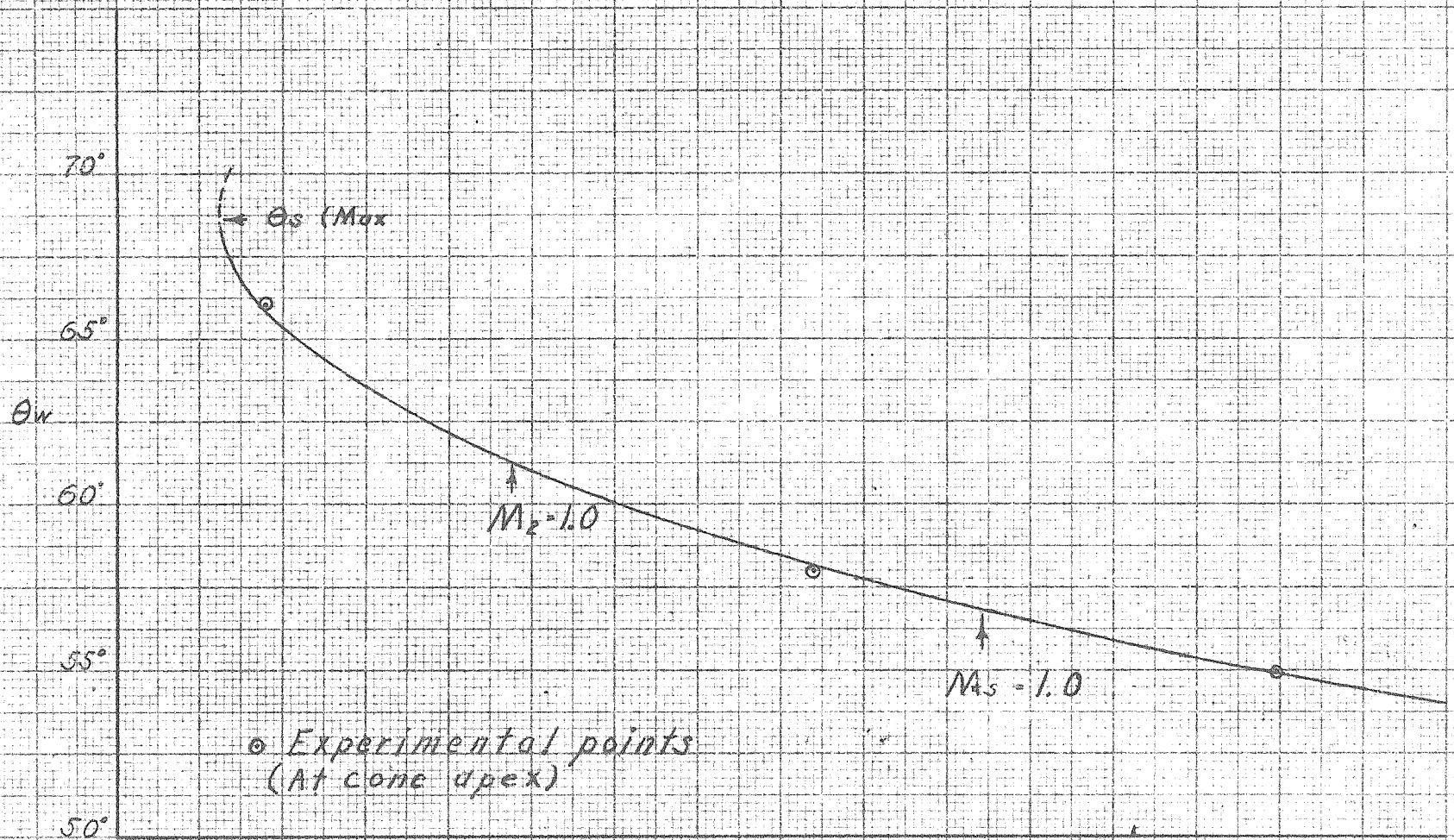

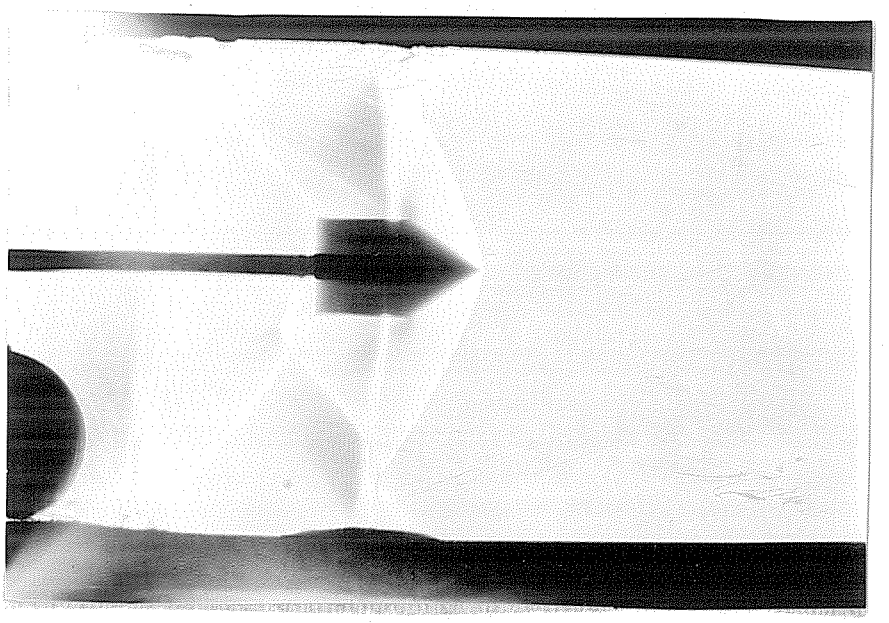

Fig. 29a

M = 1.49

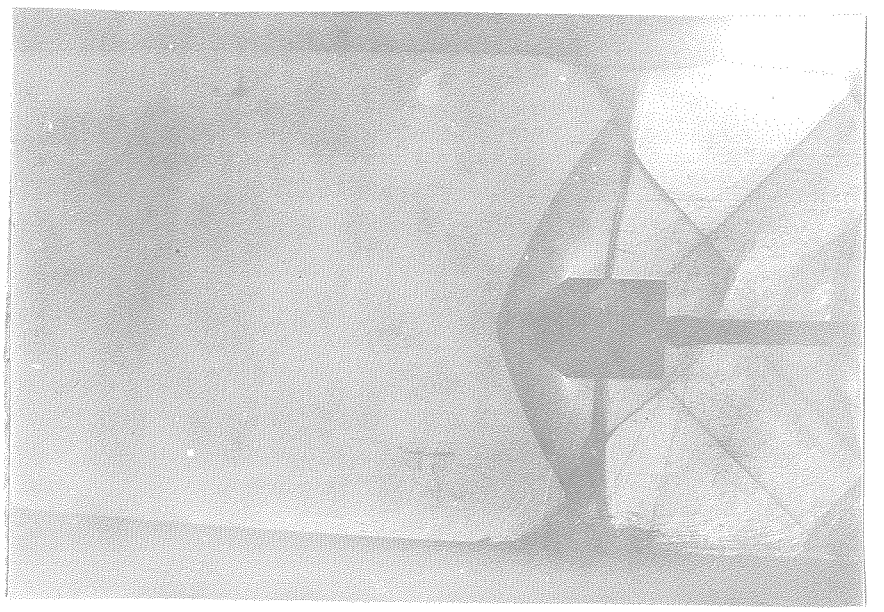

Fig. 29b

M = 1.49

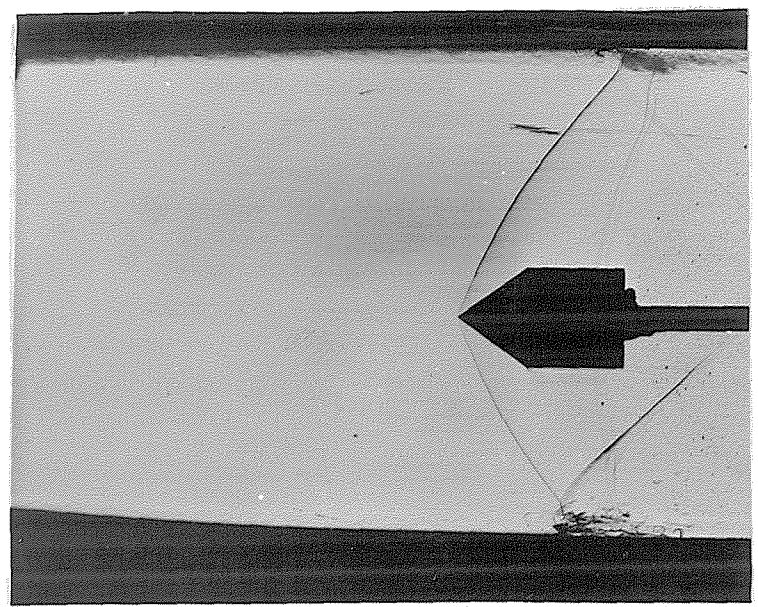

Fig. 30a

M = 1.636

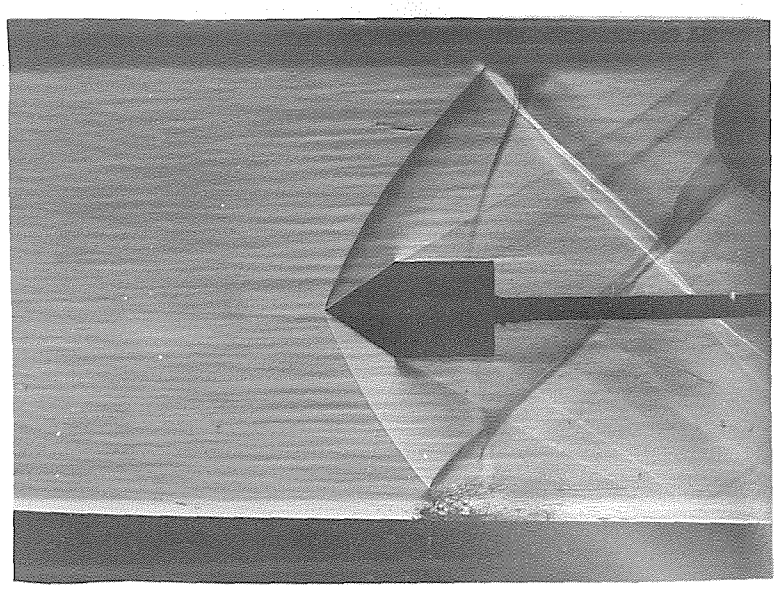

Fig. 30b

M = 1.636

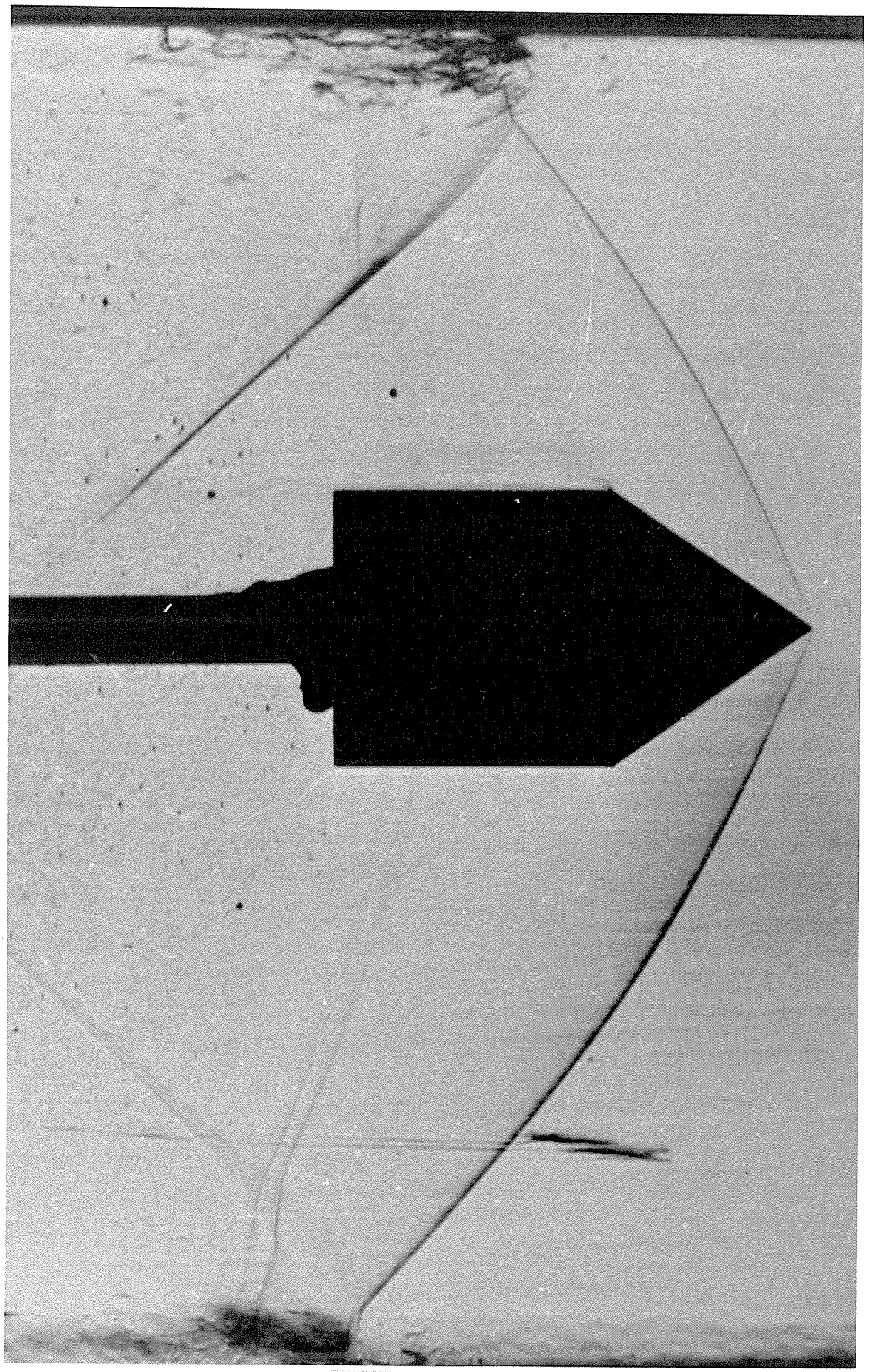

Fig. 31

M = 1.636

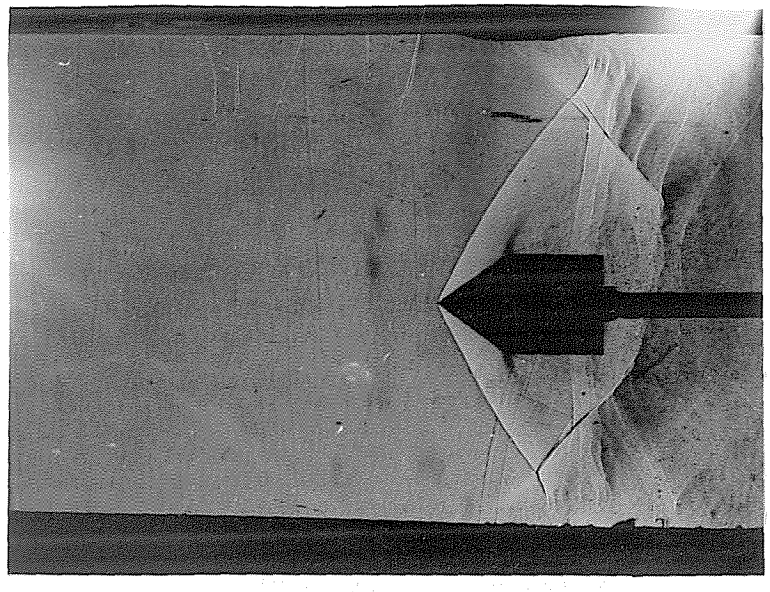

Fig. 32a

M = 1.694

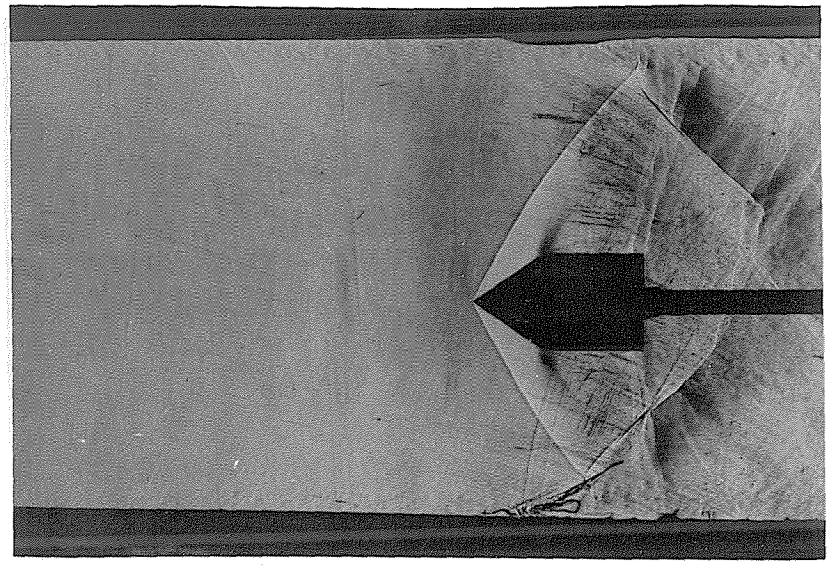

Fig. 32b

M = 1.694

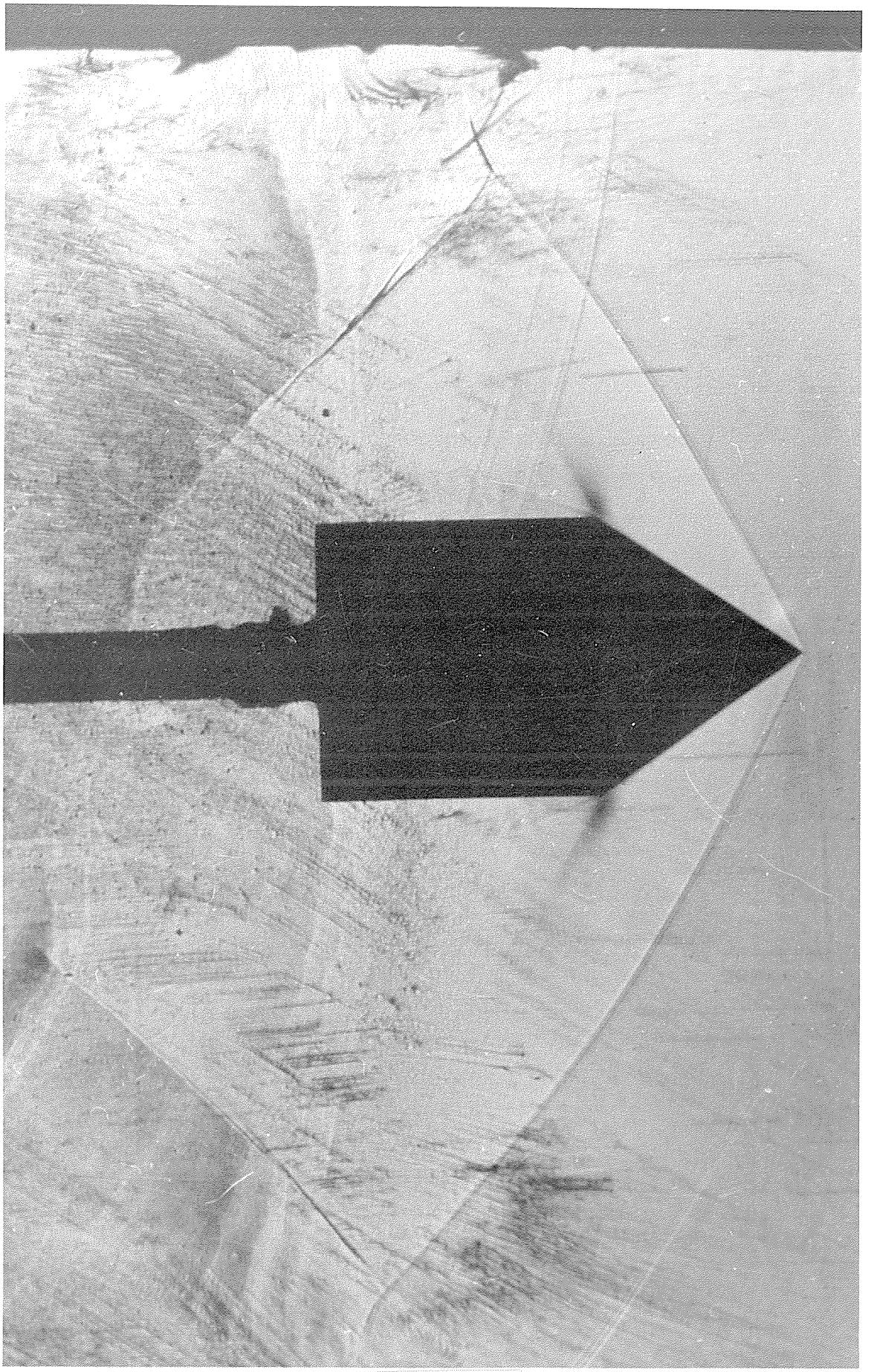

Fig. 33

M = 1.694

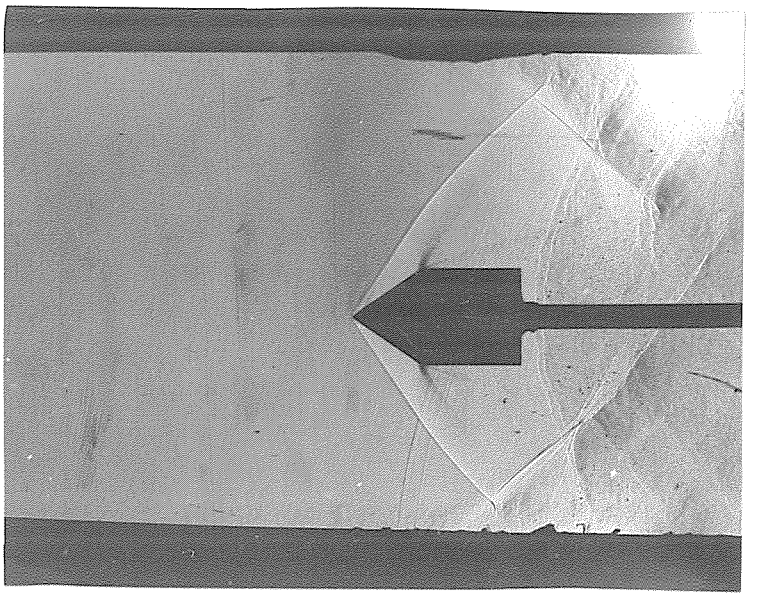

Fig. 34a

M = 1.86

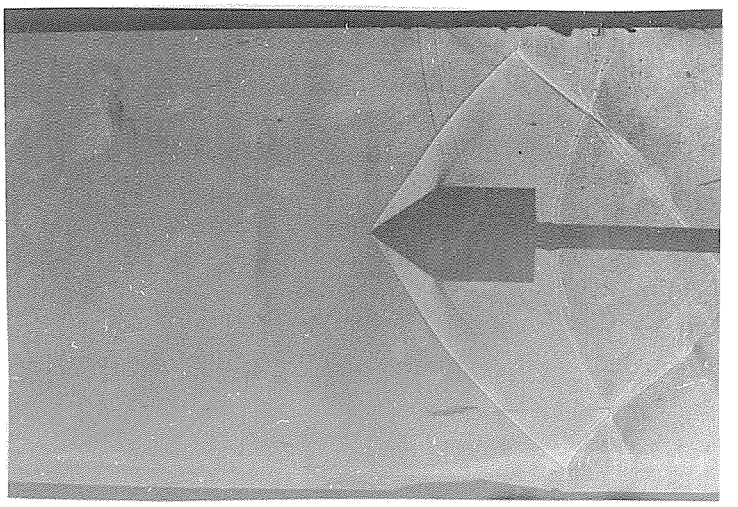

Fig. 34b

M = 1.86

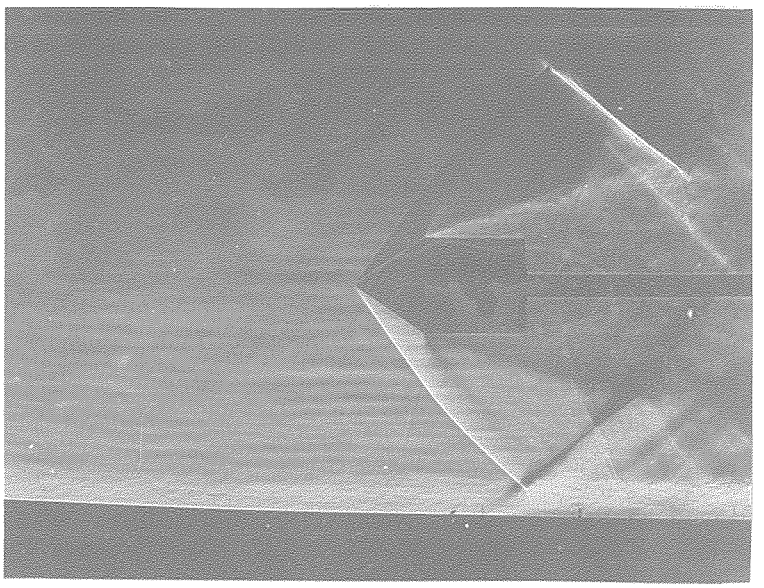

Fig. 35a

M = 1.997

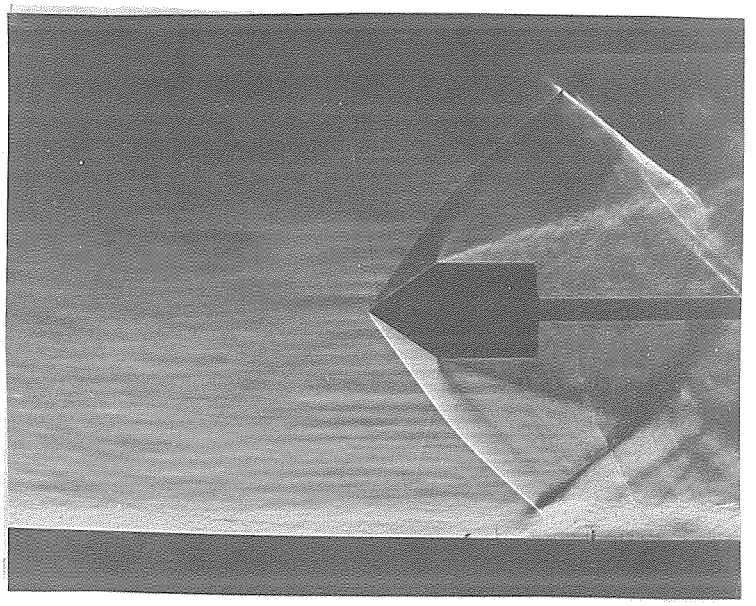

Fig. 35b

M = 1.997